Title

Deployment and Evaluation of Real-Time Vehicle Reidentification from an Operations Perspective

Authors

Coifman, Benjamin
Varaiya, Pravin

Publication Date

2002-12-01

CALIFORNIA PATH PROGRAM
INSTITUTE OF TRANSPORTATION STUDIES
UNIVERSITY OF CALIFORNIA, BERKELEY

Deployment and Evaluation of Real-Time Vehicle Reidentification from an Operations Perspective

Benjamin Coifman
Pravin Varaiya

California PATH Research Report
UCB-ITS-PRR-2002-37

This work was performed as part of the California PATH Program of the University of California, in cooperation with the State of California Business, Transportation, and Housing Agency, Department of Transportation; and the United States Department of Transportation, Federal Highway Administration.

Final Report for Task Order 4107

December 2002

ISSN 1055-1425

Deployment and Evaluation of Real-Time Vehicle Reidentification from an Operations Perspective

TO 4107 Final Report

Dr. Benjamin Coifman
Civil Engineering
470 Hitchcock Hall
The Ohio State University
Columbus, OH 43210
V: (614) 292-4282
F: (614) 292-3780
E: Coifman.1@OSU.edu

Professor Pravin Varaiya
University of California, Berkeley
Department of Electrical Engineering and Computer Science
271M Cory Hall
Berkeley, CA 94720-1770
V: (510) 642-0348
F: (510) 642-6330
E: varaiya@eecs.berkeley.edu

1 OVERVIEW

Because travel time provides information over an extended freeway link, rather than at a single point, it is a key parameter for ATIS applications and it is a powerful tool for ATMS. Under PATH sponsorship, we have already developed a prototype travel time measurement system that utilizes existing dual loop speed traps and "model 170" controllers. This research has advanced the work by improving the vehicle reidentification algorithms (Section 2), extended them to single loop detector stations (Section 3) and used the reidentified vehicles to extract both density and the net number of lane change maneuvers (Section 4). This latter work was conducted as part of the Berkeley Highway Laboratory (BHL).

2 IMPROVED VEHICLE REIDENTIFICATION AND TRAVEL TIME MEASUREMENT ON CONGESTED FREEWAYS[1]

2.1 Introduction

This Section improves upon the vehicle reidentification algorithm presented in Coifman and Cassidy (in press) for consecutive detector stations on a freeway; in the algorithm, a vehicle measurement made at a downstream detector station is matched with the vehicle's corresponding measurement at an upstream station. The work should be applicable to any detector technology capable of extracting a reproducible vehicle measurement, or *vehicle signature*. The algorithm is presented using measured vehicle lengths from conventional dual loop detectors; however it could easily be adapted to match other vehicle signatures, such as visual vehicle signatures from wayside cameras (e.g., MacCarley 1998), and vehicle dimensions from scanning laser radar (e.g., Larson *et al*. 1998).

Obviously, once a vehicle has been matched, its travel time is simply the difference in arrival times at the two stations. Travel time data could be used to improve many traffic management applications such as automatic incident detection, adaptive freeway ramp metering, and traveler information systems (Palen 1997; Balke *et al*. 1995). The data might also be used for routing vehicles over a network so as to reduce traveler delay, for calibrating traffic planning and simulation models, and for quantifying the potential benefits of emerging detector technologies that extract more detailed information from individual vehicles.

Reviewing the algorithm developed in Coifman and Cassidy (in press), it uses arrival times and number of arrivals at the upstream station to identify the set of all upstream observations in the same lane that could have come from a given downstream vehicle measurement. This set of *feasible upstream measurements* is bounded by the minimum feasible travel time between stations (the fastest possible vehicle) and an assumed maximum density (the largest number of vehicles that could be stored between the two detectors). The algorithm then takes the difference between the given downstream measurement and each of the *feasible upstream measurements*, and it identifies all pairs whose difference exceeds the measurement accuracy, as defined in the Basic Algorithm subsection below. These measurements presumably could not have come from the same vehicle, while all remaining pair-wise comparisons are treated as possible matches. Of course with this simple test the downstream vehicle will likely have many possible matches within the set, and at most, one true match amongst them. We term the collection of incorrect matches as false positives.

---

[1] E. Ergueta helped prepare this Section.

The sequence of a platoon's vehicle signatures provides more information than do the individual measurements, as is demonstrated herein. Toward eliminating false positives, the algorithm matches platooned vehicles whenever these pass both the upstream and downstream detector stations without altering their relative sequence. Obviously, lane change maneuvers disrupt these sequences, but previous research has shown that lane change maneuvers are relatively infrequent under most traffic conditions. For example, Worrall and Bullen (1970) observed that lane change frequency decreases with average velocity while Windover (1998) found that under congested conditions, consecutive vehicles will often maintain their relative order within a platoon for long distances. The algorithm has been explicitly designed to accommodate normal frequencies of lane change maneuvers (the algorithm has been tested successfully with up to 22 percent of the vehicles entering the lane between detector stations). Subsequent subsections will verify that the lane change assumptions hold for the study segments.

Using effective vehicle lengths measured by conventional dual loop detectors, the algorithm can be deployed without requiring new detector hardware. The length measurements, however, may only be accurate to half a meter due to the resolution limitations of dual loop detector data. As discussed in Coifman (1998), the accuracy of these loop detector measurements improves as vehicle velocities decrease. Consequently, for the existing detectors used in this study, the algorithm is limited to match vehicles during congested traffic conditions, i.e., when the local velocity at either station is less than 72 km/h. Coifman (in press) presents a complementary algorithm for measuring travel times from dual loop detectors during free flow traffic conditions.

Unlike the algorithm presented in Coifman and Cassidy (in press), which found a single match for each vehicle and then separately looked for patterns in these results to eliminate erroneous matches, this Section integrates the two processes. The integration makes the algorithm robust to detection errors, allowing it to identify a final match for more vehicles and to do so with higher accuracy.

The remainder of this Section is organized as follows. The first subsection summarizes our Basic Algorithm for vehicle reidentification, including how to calculate vehicle lengths from dual loop detectors, how to identify all possible matches for each downstream vehicle, and how to address lane change maneuvers. The second subsection describes the new work done to eliminate false positives, which includes the development of four independent tests. The third subsection applies the algorithm over large data sets. The final subsection presents concluding remarks.

2.2 The Basic Algorithm

The vehicle reidentification algorithm is described here via its application; i.e., it is applied to traffic data measured in a single lane at two neighboring dual loop detector stations, 0.55 km apart, in the Berkeley Highway Laboratory along Interstate-80, north of Oakland, CA (Coifman *et al*. 2000).

2.2.1 Vehicle Length Measurement

The first step in the algorithm is to measure vehicle lengths. To illustrate this process, Figure 2-1A shows a time-space diagram depicting a vehicle passing over a dual loop detector. The controller normally records four transitions, i.e., the turn-on and turn-off times at each of the loops, as shown in Figure 2-1B. These measurements are used to calculate: dual loop traversal time via the rising edges, TT_r, dual loop traversal time via the falling edges, TT_f, total on-time at the first loop, OT_1, and total on-time at the second loop, OT_2, as indicated in the figure.

Occasionally a vehicle will change lanes over the dual loop detector or one of the loop detectors will malfunction and these misdetections will impact the performance of the reidentification algorithm. For the data presented in this study, less than three percent of the data collected presented these errors. Figures 2-2A-B and 2-2D-E show the most common errors at a dual loop detector. It can be difficult to differentiate between flicker at one loop and the other loop failing to detect a vehicle, but both errors result in two sequential pulses at one loop without an intervening pulse at the other loop. The algorithm in Coifman and Cassidy (in press) discarded all of the questionable pulses, i.e., those highlighted with gray rectangles in Figure 2-2. As a result, this cleaning process discarded one or two vehicles whenever an error occurred. However, comparing Figures 2-2A and 2-2B, regardless of which error occurs, two parameters are always measured correctly, OT_2 and TT_f. We now keep the pulse at the second loop and use these measurements to reconstruct a pulse at the first loop by retaining TT_f and setting OT_1 equal to OT_2, as shown with dashed lines in Figure 2-2C. Looking at Equation 2-1 below, it becomes clear that equating OT_1 to OT_2 implicitly assumes that the vehicle passes both loops without accelerating, which is a reasonable assumption due to the small spacing (6.1 m) between the dual loops. The analogous process of reconstructing a pulse at the second loop is shown in Figures 2-2D-F. The improved cleaning process will still sometimes discard a vehicle, but to the vehicle reidentification algorithm these missing pulses simply appear to be a phantom vehicle that entered or exited the lane between the stations.

Obviously, the loop separation (6.1 m in this case) divided by the traversal time yields the vehicle velocity. It is clear from Figure 2-1A that two measurements are available for the effective vehicle length,

$$\begin{aligned} length\,measurement\,\#1: \qquad & L_1 = 6.1\frac{OT_1}{TT_r}\,[m] \\ length\,measurement\,\#2: \qquad & L_2 = 6.1\frac{OT_2}{TT_f}\,[m] \end{aligned} \tag{2-1}$$

and the algorithm uses the average of the two. Equation 2-1 and Figure 2-1A show that the effective vehicle length is the sum of the physical vehicle length and the length of the detection zone.

Since the controller samples the loops at 60 Hz, the traversal times and on-times in Equation 2-1 are accurate to ±1/30 seconds. To capture this resolution constraint, the measurement uncertainty is defined as the range spanned by [L_1, L_2] after including ±1/60 seconds in OT_1, OT_2, TT_r and TT_f. To ensure the accuracy of OT_1, OT_2, TT_r *and* TT_f, any hardware problems at each station, such as cross talk between detectors, were identified using Coifman (1999) and corrected.

2.2.2 Possible Matches and the Vehicle Match Matrix

Within each lane, vehicles are assigned successive arrival numbers as they pass each detector station and these numbers are assigned independently at each station. Next, a set of *feasible upstream measurements* is identified for each downstream measurement, as discussed previously. The algorithm finds all vehicles in this set with a length range that intersects that of the downstream vehicle. The results of this resolution test (i.e., the set of possible matches for each downstream vehicle) are stored as one row in a matrix termed the vehicle match matrix (VMM). Figure 2-3 shows the VMM for 100 downstream vehicles, where each point represents a possible match. Note that the columns are indexed by the difference between the arrival numbers assigned to vehicles at the upstream and downstream detector stations (upstream offset). Therefore, each diagonal in the VMM corresponds to all possible matches for a given upstream vehicle. Note that throughout this Section, a diagonal in the VMM will refer to a diagonal going from the upper right to the lower left corner of this matrix.

The false positives are randomly distributed over the VMM, but if vehicles usually maintain their order between stations (i.e., assuming lane change maneuvers are relatively infrequent), the true (but unknown) matches should manifest themselves as sequences of possible matches in the same column. For simplicity, the term sequence is used to refer to a sequence of possible matches in the same VMM column. So in other words, false positives will typically form short sequences in the VMM's columns while true matches will usually form longer sequences within single columns.

After discussing lane change maneuvers, several tests are developed that exploit this property to eliminate false positives. After applying these tests, each downstream vehicle is matched to at most one upstream vehicle. Some of the tests explicitly look for a small set of lane change maneuvers, as discussed below.

2.2.3 Lane Change Maneuvers and Best Matches

After finding sequences of possible matches in the VMM, the reidentification algorithm searches for a small set of lane change maneuvers between sequences as outlined in Coifman and Cassidy (in press). Although the algorithm does not attempt to match vehicles that have changed lanes, these maneuvers impact the relative order of the vehicles that remain in the lane, and the algorithm must correct for these changes. Briefly summarizing the process, Figure 2-4A-C respectively show the three maneuvers searched for: a vehicle exiting a lane, a vehicle entering a lane, and a vehicle entering a lane while another exits the same lane. For each new sequence of possible matches, the algorithm checks to see if it can be linked to an earlier sequence via one of the maneuvers. This search is only applied to the first match in the sequence, downstream vehicle m in this example, and the algorithm looks at the neighboring columns for two preceding downstream vehicles, the shaded elements in Figure 2-4D. When a possible lane change occurs, the algorithm joins the two sequences in a *modified sequence*, as illustrated in Figures 2-4E-F. Except where noted, these *modified sequences* include at most a single lane change maneuver, but a given possible match that is included in a sequence may be included in many *modified sequence*s. Note that the set of *modified sequences* includes all of the original sequences as well. The Basic Algorithm will select the longest *modified sequence* from this set, so that for each row, the algorithm finds the element corresponding to the maximum value (*best match*), thus, identifying the longest *modified sequence* for a given downstream vehicle.

Provided traffic does not stop over one of the detectors, the link travel time usually will not change significantly between two successive vehicles. In the event that there is a tie for the *best match* in a row of the VMM, the algorithm will compare the resulting travel times for each of the matches from this set to the median travel time of the previous 30 vehicles already matched. If the local velocity measurements indicate that traffic has not recently stopped over one of the detectors, the algorithm will eliminate all of the matches from the set that have a travel time more than 20 seconds different from the median. If more than one match still remains in the set, none of them will be retained as a *best match*. Except for these rare cases, the algorithm will yield a single, unique *best match* for each downstream vehicle. Figure 2-5 shows an example of the resulting matches from the Basic Algorithm (including lane change maneuvers), applied to the VMM of Figure 2-3. A few obvious false positives remain in this example between columns 20 and 55, and also around

column 90. The next subsection will attempt to improve performance by further eliminating these false positives as well as others that are not as obvious to the eye.

2.3 Tests to Eliminate False Positives

Four tests have been developed to improve the performance of the Basic Algorithm, as described below. The Filter and Cone Tests are applied before searching for lane change maneuvers (starting from the original VMM matrix) while the Multiple Lane Change Test is applied concurrently with this search and the Travel Time Test is applied after this search (since it needs a preliminary "best match" for each downstream vehicle). Each test is designed to run independent of the other tests.

2.3.1 Filter Test

As previously discussed, true matches tend to form longer sequences than false positives do. This test will favor areas of high density of matches in the VMM. The Filter Test uses aggregate trends to narrow the range of *feasible upstream matches* to a small number of columns in the VMM that are most likely to contain the true matches. So, as opposed to the upcoming tests, the Filter Test does not look for final matches, but for a "final region."

The Filter Test starts with the VMM and selects all matches that are members of the three longest vertical sequences for each row and for each diagonal, i.e., the most promising matches for a downstream vehicle and an upstream vehicle, respectively. Figure 2-6A shows an example of this *pre-selection* applied to the VMM of Figure 2-3. The Filter Test will ignore matches if they fall in sequences shorter than five vehicles.

The remaining matches are assigned a weighting of "1", and all other elements in the matrix are assigned a weighting of "0" (blank spaces in the figure). Most vehicle lengths fall within a small range; the remaining vehicles (about ten percent for the subject location) are distinct and have fewer false positives associated to them. Exploiting this fact, if a downstream vehicle has a possible match for less than 10 percent of its feasible matches, the vehicle's weighting will be doubled. The Filter Test also favors matches that fall in longer sequences (i.e., situations with no detected lane change maneuvers). Specifically, if a match belongs to a sequence that is 1.25 times longer than the median sequence length passing through the row of the VMM, the match 's weighting is also doubled. Thus, a distinctive vehicle in a long sequence may ultimately receive a weighting of "4".

Each element of the filtered VMM now has a weighting of 0, 1, 2 or 4. Next, the Filter Test takes a moving average of 20 rows within each column, i.e., for each element in the filtered VMM, it calculates the mean weighting over the previous 20 elements in the same column. Once more,

assuming that true matches usually form longer sequences than false positives, this process should favor the former. Comparing Figures 2-6A-B, this averaging has extended the sequences. Although it is not shown in Figure 2-6B, each of the matches has a different weighting associated with it. Also note that the small sequences (shorter than five vehicles long) that are shown in Figure 2-6A have been discarded in a previous step, and therefore do not appear in Figure 2-6B.

Under most traffic conditions true matches usually will not change columns rapidly because, as previously noted, each column shift represents the relatively infrequent lane change maneuvers. This property is evident in the higher density of matches shown around column 82 in Figure 2-6A. Taking the results from the vertical moving average (Figure 2-6B), the Filter Test then calculates a moving average of five columns within each row in order to "connect" sequences from adjacent columns of the filtered VMM and account for lane change maneuvers. The results of this horizontal moving average represent the final weightings for each element in the filtered VMM.

Next the Filter Test selects all matches that have a weighting greater than a threshold. In the present study, to determine this threshold we calculated the mean over all non-zero final weights from the filtered VMM. The threshold was then set to 5 times this mean weighting. The averaging and thresholding process is repeated a second time to further narrow the set of possible matches. Everything that remains defines the *good region*, e.g., Figure 2-6C.

Even though determining the *good region* is the ultimate goal of the Filter Test, in order to appreciate its performance, we apply the Basic Algorithm to the same VMM independently of this test. Finally, only the intersection of the best matches from the Basic Algorithm (Figure 2-5) and the *good region* from the Filter Test (Figure 2-6C) are retained as final matches for this test, e.g., Figure 2-6D.

2.3.2 Cone Test

Although the true matches are not known a priori, they will usually be preceded by other true matches in nearby columns. The Cone Test will favor patterns of matches that resemble earlier true matches. This test uses coarse information to narrow the set of possible matches in the VMM, starting once more with the matches that fall in the three longest sequences per row and diagonal in the VMM, e.g., Figure 2-6A. This test considers each of the resulting sequences individually, unlike the Filter Test. For the first element of each sequence, the algorithm considers a "cone" of earlier matches expanding upwards from the match, e.g., the shaded area in Figure 2-7A. The cone spans 20 rows, with the left-hand boundary corresponding to the situation where every other vehicle enters the lane, and the right-hand boundary corresponding to the situation where every

other vehicle exits the lane. Since entering and exiting vehicles result in different column shifts, as shown in Figure 2-4, the cone is asymmetric.

In this manner, it is assumed that any matches below the cone can not precede the given sequence via lane change maneuvers, but those within the cone could have. Thus, if a sequence exits the bottom of the cone, all matches below the cone will be excluded from that sequence's length, e.g., a sequence containing two matches within the cone and five below the cone will be treated as if it only has two matches for the given cone. On the other hand, the length for a sequence starting above the cone will include all of the matches above the cone since they could still precede the possible match at the vertex of the cone, e.g., for a sequence containing 13 matches, starting above the top of the cone and ending inside the cone, all 13 matches will be included.

A *cone weight* is calculated for each new sequence, based on the sum of the lengths of all sequences within the cone. For example, for a cone containing two sequences, one composed of 13 matches and the other of 2 matches, the resulting *cone weight* would be 13+2=15.

As in the previous test, the Cone Test favors unique vehicles that are likely to have fewer false positives, and therefore the *cone weight* is increased by one unit for each match within the cone that corresponds to an uncommon vehicle length, i.e., if a downstream vehicle has a possible match for less than 10 percent of its feasible matches. Also, if any match in the cone belongs to an unusually large sequence compared to the other matches for that row of the VMM (at least 1.25 times the median sequence length passing through the given row) the *cone weight* is increased by 5 units per long sequence.

After calculating the *cone weight* for each sequence, the test selects only the sequences that have a *cone weight* of at least 0.75 times the average *cone weight* over the preceding 50 rows of the matrix. The results of this selection are shown in Figure 2-7B. Some rows may still contain more than one match at this stage, so the remaining sequences are joined vertically by lane change maneuvers and the longest *modified sequence* passing through a given row is retained. The final matches from the small example are shown with dark circles, superimposed on the original VMM, in Figure 2-7C.

2.3.3 Travel Time Test

As previously noted, two successive vehicles will usually have similar link travel times unless one of them comes to a stop over one of the detector stations. The Travel Time Test exploits this property to eliminate false positives and when possible, finds a more promising match for a given downstream vehicle. This test starts with the *best matches* from the Basic Algorithm and considers

each of these matches one at a time, processing them in the order of the downstream vehicle numbers (going top to bottom in the matrix in Figure 2-5). First the test discards any match indicative of a vehicle traversing the link at a very high velocity. For the present study, any vehicle moving faster than 120 km/h would be discarded. If a match passes that step, the resulting travel time is compared to that of the median travel time over all final matches (matches that have already passed this test) in the 30 preceding rows. If this travel time is within 20 seconds of the median, the match will be retained. Otherwise, the Travel Time Test examines the local velocities at the two detector stations to see if a passing disturbance could explain the difference in travel times. In the event of such a disturbance, consecutive vehicles should still have similar upstream offsets, i.e., fall in or near the same column of the VMM. So, a match will also be retained if such a disturbance passed one of the detectors and the upstream offset for the subject match is within five columns of the median upstream offset over all final matches in the 30 preceding downstream vehicles.

Since the local travel time median only includes matches that have previously passed this test, a match will also be retained in the event that there are fewer than 10 matches in the set because such set is considered too small to yield meaningful conclusions. For this reason, the last matches in a very long sequence of false positives might be retained. For example, a long sequence of false positives is shown with points in column 20 of Figure 2-8A. The first few matches in this sequence are discarded, but eventually the test retains the end of the sequence (shown with light circles). By the same mechanism, the test will recover from such errors after discarding a few true matches. Again, notice in Figure 2-8A that even though the first few matches of the true sequence in column 80 (starting at row 150) are not retained by the test, the rest of the sequence is.

If the match for a downstream vehicle fails to pass these steps, the Travel Time Test will then attempt to find a better match for that vehicle by checking the second and third longest sequences in the row. These matches will only be considered if they are also among the three longest sequences for the given diagonal, e.g., Figure 2-6A. Out of this set, the match with the smallest difference from the median travel time will be retained provided it is within 20 seconds of the median, as before. The final matches from the small example are shown with dark circles, superimposed on the original VMM, in Figure 2-8B.

2.3.4 Multiple Lane Change Test

The Multiple Lane Change Test is based on the identification of possible lane change maneuvers as explained in the Basic Algorithm subsection. Rather than only finding *modified sequences* linked by a single lane change maneuver, this test processes the VMM five separate times, each time allowing for *modified sequences* containing one additional lane change maneuver than the previous

pass, up to a total of five lane change maneuvers. Figure 2-9A compares the *best matches* when a single lane change maneuver is allowed against those when five lane change maneuvers are allowed. Note the differences around rows 37, 53 and 99.

This test is based on the observation that the various number of lane change maneuvers will be vulnerable to different errors. For example, a long sequence of false positives is more likely to corrupt the algorithm when only single lane change maneuvers are considered. On the other hand, many short sequences of false positives might be joined together and corrupt the algorithm when it allows multiple lane change maneuvers. The true matches, however, should be consistent across the different number of lane changes.

For each of the five cases, the test selects the matches that are members of the five longest *modified sequences* per row and diagonal. Then, the intersection of these sets is generated. This intersection is treated like a new VMM and then processed using the same steps as in the Basic Algorithm, i.e., after allowing for a single lane change maneuver between sequences of matches, the test finds the element corresponding to the longest *modified sequence* in the row or *best match*. The final matches from the small example are shown with dark circles, superimposed on the original VMM, in Figure 2-9B.

Obviously the previous tests include several parameters. Additional testing over a wide range of locations would be necessary to optimize these values. At present the 60 Hz detector data used in this study are not widely available and securing such data is the subject of ongoing work. Meanwhile, the values used in this Section provided successful results in all 10 lanes in each of the six links of the Berkeley Highway Laboratory.

2.4 Results

To illustrate the performance of the new tests, they are applied to two different scenarios. The first scenario corresponds to an hour of data collected from the same lane at two detector stations 0.55 km apart, with no ramps between them. The second scenario corresponds to a two-hour period of data collected for all lanes at two detector stations also 0.55 km apart, but this time with an off ramp in between them.

For the first scenario video data were also colleted at these stations and all vehicles that passed during the study period were visually matched between the two locations. In this sample, 1,462 vehicles passed the downstream station, out of which, 193 entered the lane between the detectors and did not have a match. The resulting travel times for the remaining 1,269 vehicles were calculated. Figures 2-10A-D show the resulting travel times for the matches extracted by each of

the tests (light X's) contrasted against these ground truth travel times (dark line). Table 2-1 summarizes the number of matches found by each of these tests. The first column includes all the final matches shown in Figures 2-10A-D, including some that fall outside the region for which we have ground truth data. The remaining columns of the table reflect only the matches found within the period for which ground truth data are available.

Although all of the tests retain a few false positives, the selection mechanisms are different and each test keeps a different set of false positives. This property is exploited to further eliminate errors by running all these tests in parallel and retaining only those matches that appear in at least two of the tests. Figure 2-10E shows the resulting travel times for the sample of 1,462 vehicles contrasted against the true travel times, and the number of matches is also reported in Table 2-1. Applying a modified version of the Travel Time Test to the matches, as explained momentarily, further improves the results. Now, however, if the travel time associated with a vehicle is not within one minute of a local travel time median (considering the previous 20 vehicles) the current match is discarded. Figure 2-10F and Table 2-1 show the results after applying this final filter for the same sample of 1462 vehicles. As is evident by the travel times Figure 2-10F and Table 2-1, most of the incorrect matches are very close to the true match for those vehicles.

In general the *new algorithm* performs significantly better than the *old algorithm* from Coifman and Cassidy (in press). These differences are particularly apparent when large numbers of vehicles enter or exit the lane. The second scenario considers just such a case, matching vehicles in a segment that includes an off-ramp between the detector stations. Unlike the first scenario, this example considers all five lanes and compares the results from both the *old* and *new algorithms*.

Once more we use video collected concurrently with the loop data to verify the performance of the algorithms. It would be prohibitively time consuming to manually match the 13,500 vehicles that passed both detector stations during this example. Fortunately, it is not necessary to match every vehicle manually. If the algorithm is correctly matching vehicles, it will also yield the true travel times for those vehicles. Although travel time over a freeway link can change dramatically in a short period of time, the travel times for two successive vehicles will be very similar. Thus, a human observer must manually match a sufficient number of vehicles to capture changes in link travel time, but this can be accomplished using a small fraction of the passing vehicles. We matched an average of two vehicles per minute for verification in this scenario.

Figure 2-11 shows the travel times of all the vehicles in the second scenario matched by the *new algorithm* contrasted against the manually generated matches. The equivalent link velocities ranged from free flow down to 6 km/h during this example. Similar accuracy was found with the *old*

algorithm, although the frequency of matches was considerably lower. As shown in Table 2-2, in some lanes the *new algorithm* matched more than twice as many vehicles as its predecessor did.

In the first scenario the new algorithm matched 86 percent of the vehicles while in the second scenario it recognized between 35 and 65 percent of the vehicles that passed both detector stations, depending on the lane. The required matching rate depends on the ultimate application. For example, Van Aerde *et al*. (1993) estimated that matching 20 percent of the population is sufficient for travel time measurements, and Holdener and Turner (1996) suggests that the percentage may be even smaller. Clearly, the algorithm has surpassed these requirements in both scenarios.

2.5 Conclusions

This Section has presented an algorithm to match a vehicle's length measurement at a downstream detector station with that vehicle's corresponding measurement at an upstream station. Although this algorithm is potentially compatible with many vehicle detector technologies, the Section illustrated the method using existing dual loop detectors to measure vehicle lengths. Of course once a vehicle has been matched across neighboring detector stations, the difference between its arrival times at each station defines the vehicle's travel time on the intervening segment.

The algorithm rules out unlikely matches, looks for sequences of possible matches between measurements at the two stations, and then eliminates unlikely sequences of these matches. This elimination process is based on the assumptions that lane change maneuvers are relatively infrequent, sequences of true matches tend to be larger than those of false positives, and that two successive vehicles will usually have similar link travel times. These assumptions were used to develop four tests to eliminate false positives: Filter Test, Cone Test, Travel Time Test, and Multiple Lane Change Test. Although none of the tests are perfect, they all produce good results and as illustrated, the results can be improved by combining the tests because they exhibit different errors. Meanwhile, ongoing research is seeking to optimize the parameters used in these tests.

The beauty of our approach is its simplicity and its low cost, since our research is completely compatible with the hardware (for detection and communication) that some operating agencies have already deployed, such as those in California, Ohio and Massachusetts. Several other algorithms have been proposed for measuring travel time directly using improved vehicle signatures, such as Reijmers (1979), Pfannerstill (1984), Kuhne and Immes (1993), and Huang and Rusell (1997). These algorithms, however, require the deployment of new detector infrastructure even before the benefits of measuring travel time can be quantified. Other surveillance systems, such as Dailey (1993), Petty (1997), Westerman and Immers (1992), and Westerman *et al*. (1996), have been

proposed for the estimation of travel time, but these systems currently perform poorly under heavy congestion. Our work is among the few methods that can accurately measure travel time with the existing surveillance infrastructure during congested conditions.

Finally this work represents a significant improvement over our preceding work, Coifman and Cassidy (in press). We not only increased the number of vehicles matched, but also obtained accurate travel time measurements with an off-ramp between the detector stations and a higher frequency of lane change maneuvers.

Figure 2-1 One vehicle passing over a dual loop detector, (A) the two detection zones and the vehicle trajectory as shown in the time space plane. The height of the vehicle's trajectory reflects the non-zero vehicle length. (B) The associated turn-on and turn-off transitions at each detector.

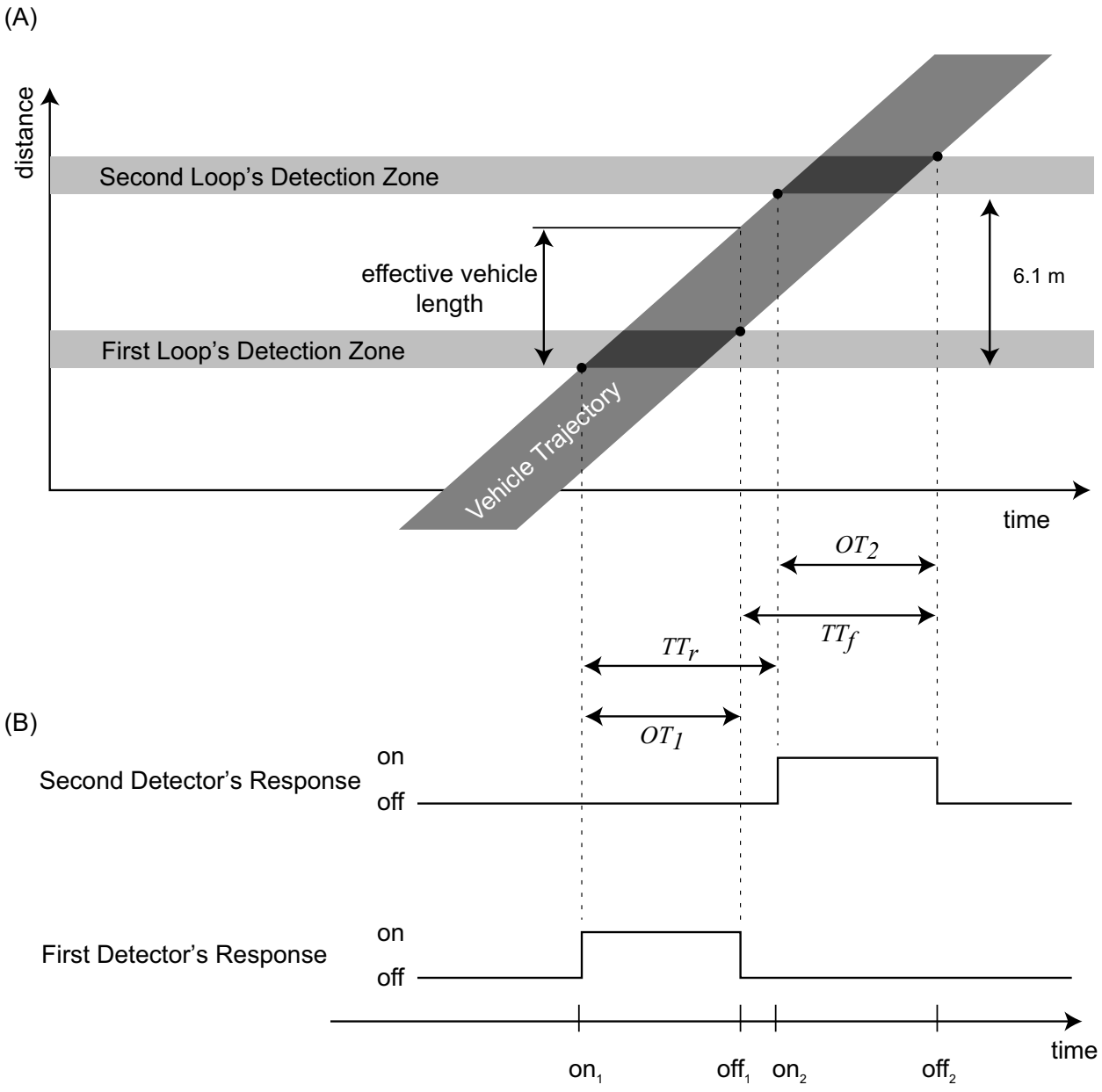

Figure 2-2 Analysis of detection errors between paired loops, (A) the first loop flickers as a vehicle passes, (B) the second loop fails to detect a vehicle, (C) regenerated pulse at the first loop, (D) the second loop flickers as a vehicle passes, (E) the second loop fails to detect a vehicle, (F) regenerated pulse at the second loop.

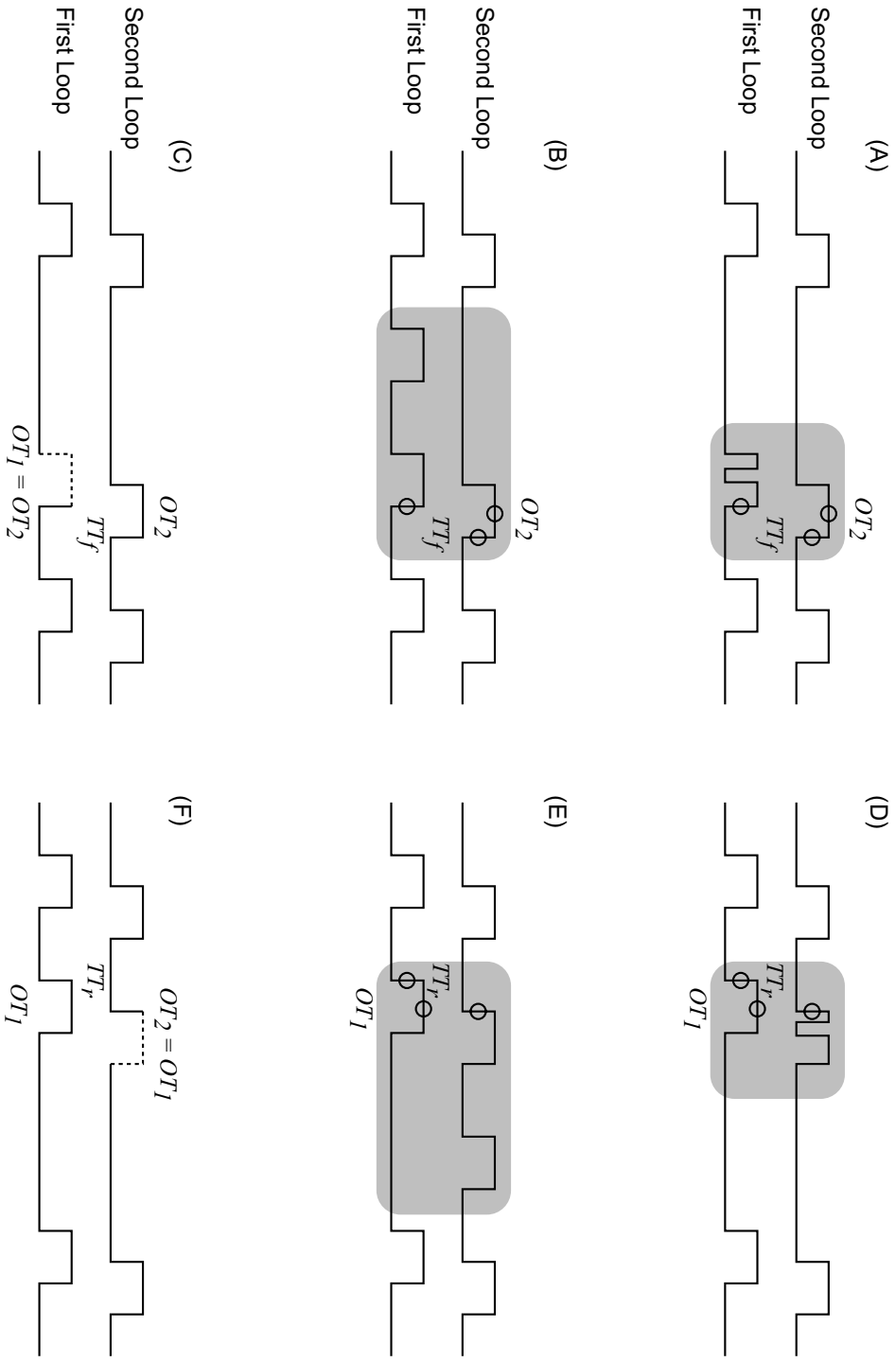

Figure 2-3 A sample VMM for 100 downstream vehicles.

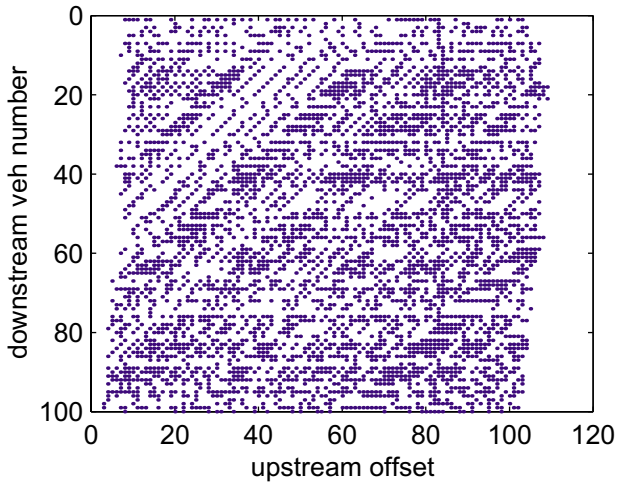

Figure 2-4 A simple example illustrating the possible disruptions recognized by the Algorithm: (A) One vehicle exits the lane between stations or is not detected downstream, (B) One vehicle enters the lane between stations or is not detected upstream, (C) One vehicle enters and one vehicle exits the lane between stations or is measured incorrectly at one of the stations, (D) The search region for the sequence starting at element (m,n). (E) Three sample sequences, one in each column n-1 to n+1. (F) In this case, the sequence starting at (m,n) is joined via an entrance (part B) to a portion of an earlier sequence.

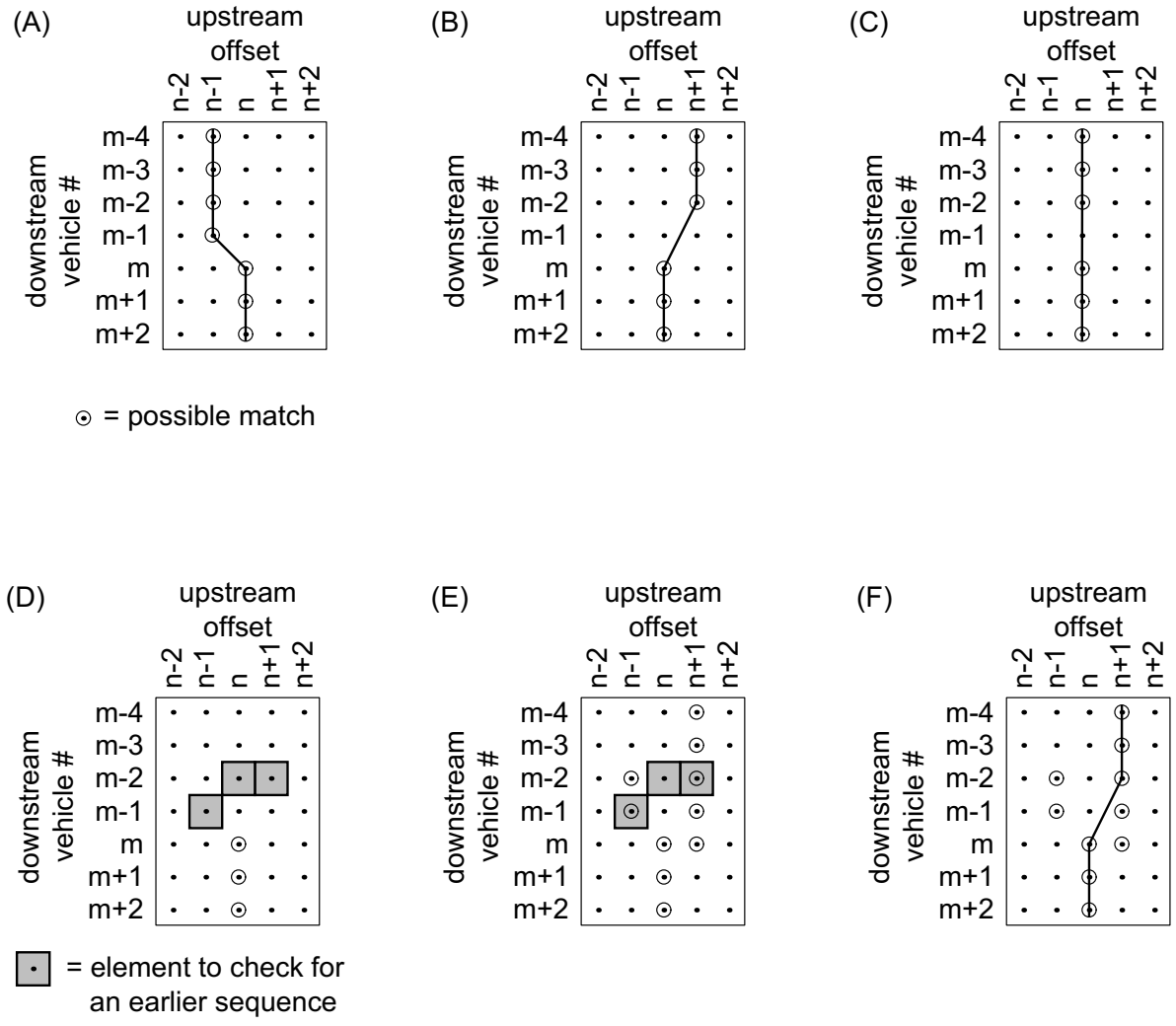

Figure 2-5 Matches (circles) after accounting for lane change maneuvers and initial VMM (light points).

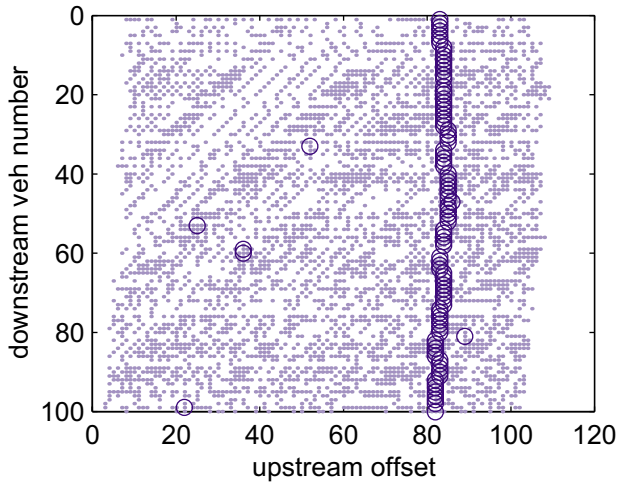

Figure 2-6 (A) Selection of best 3 matches per row and diagonal before lane changes, (B) extended sequences after vertical moving averages, (C) good region, (D) final matches (circles), possible matches within good region (dark points), and initial VMM (light points).

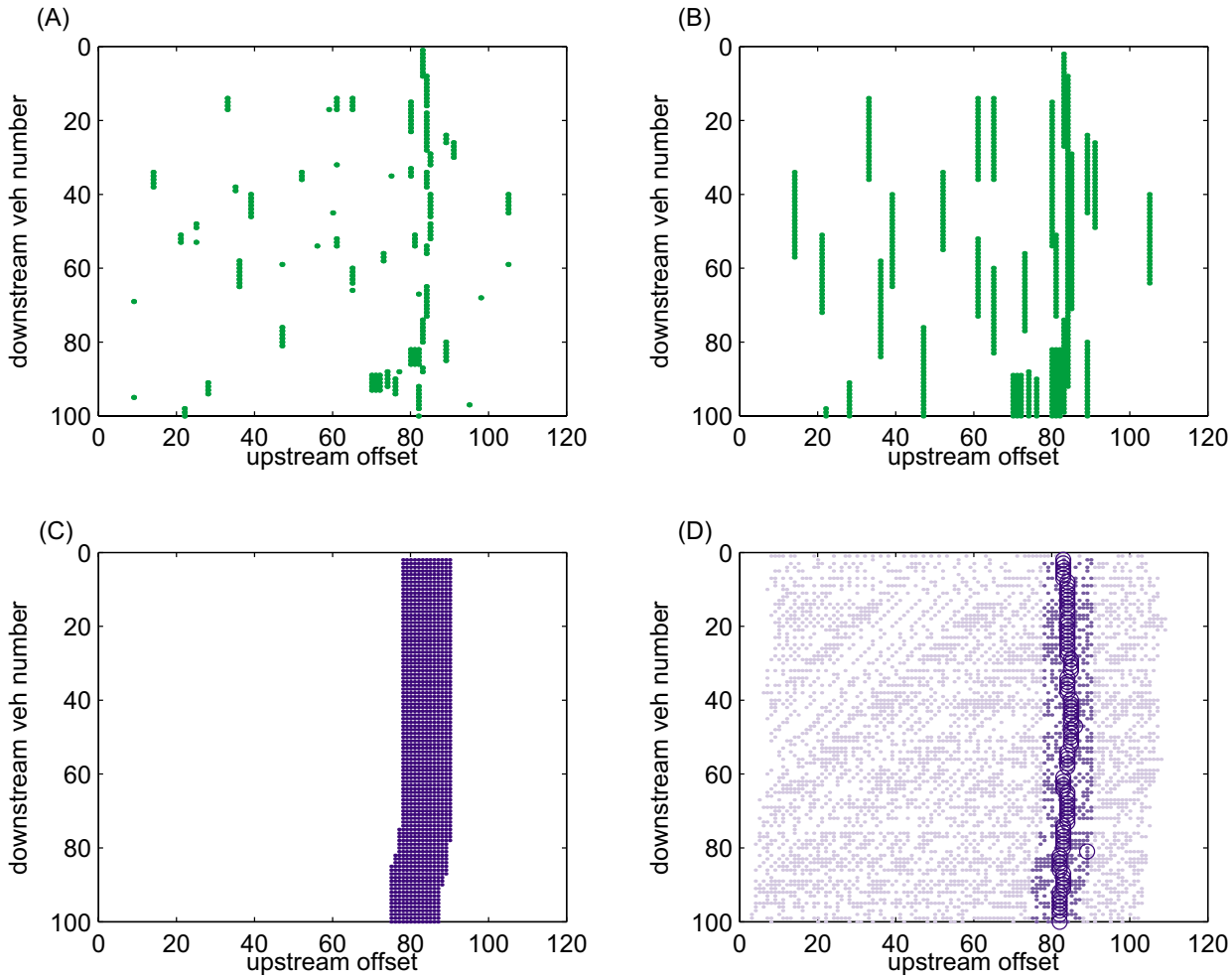

Figure 2-7 (A) Construction of a cone, (B) sequences that passed the test, (C) final matches (dark circles) and the original VMM (light points).

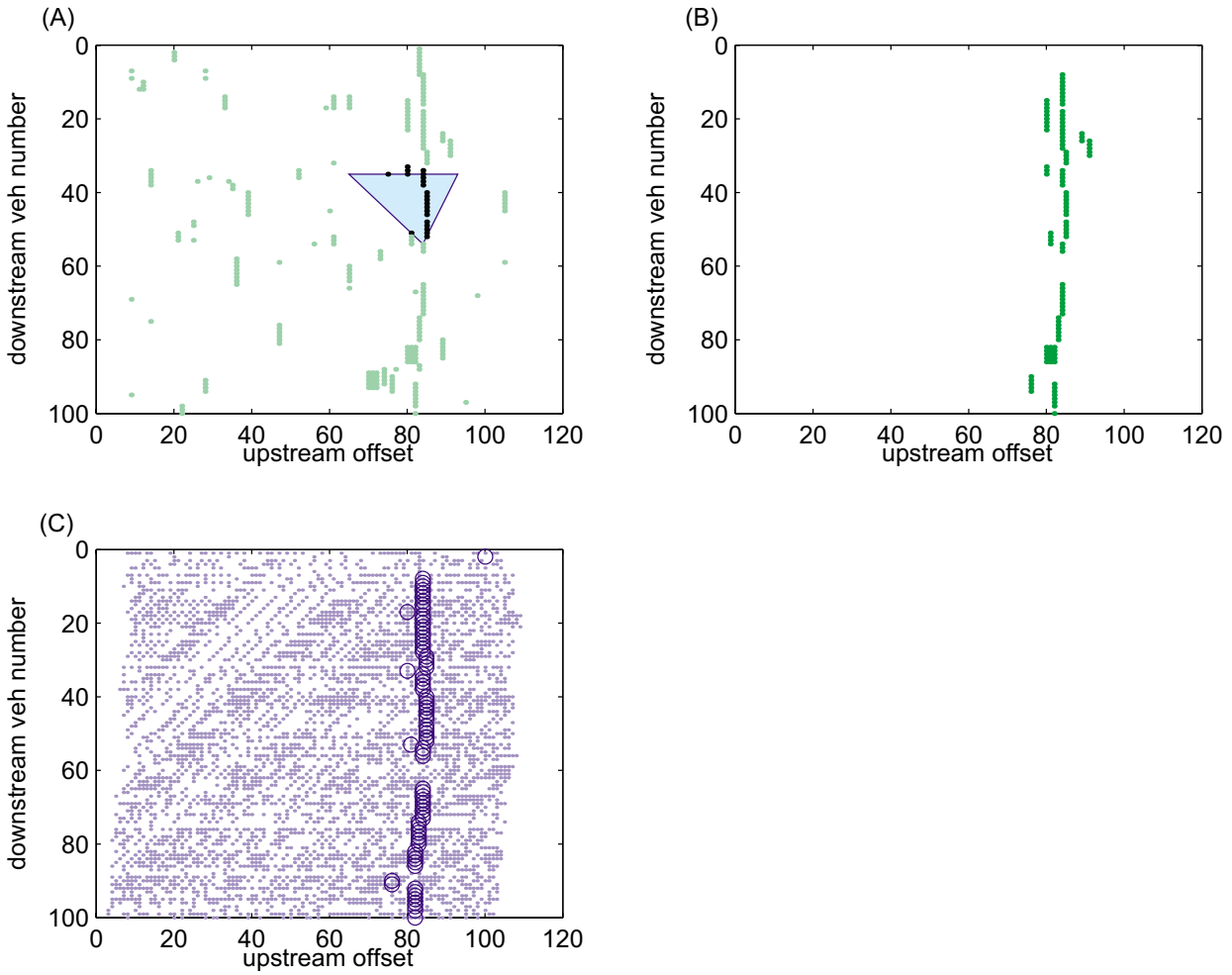

Figure 2-8 (A) An example of the Travel Time Test recovering after a long sequence of false positives, dark points indicate possible matches from the Basic Algorithm and light circles are those matches selected by the test at this step (note this matrix does not correspond to the data shown in Figure 2-3), (B) final matches (dark circles) and the original VMM (light points) from the data shown in Figure 2-3.

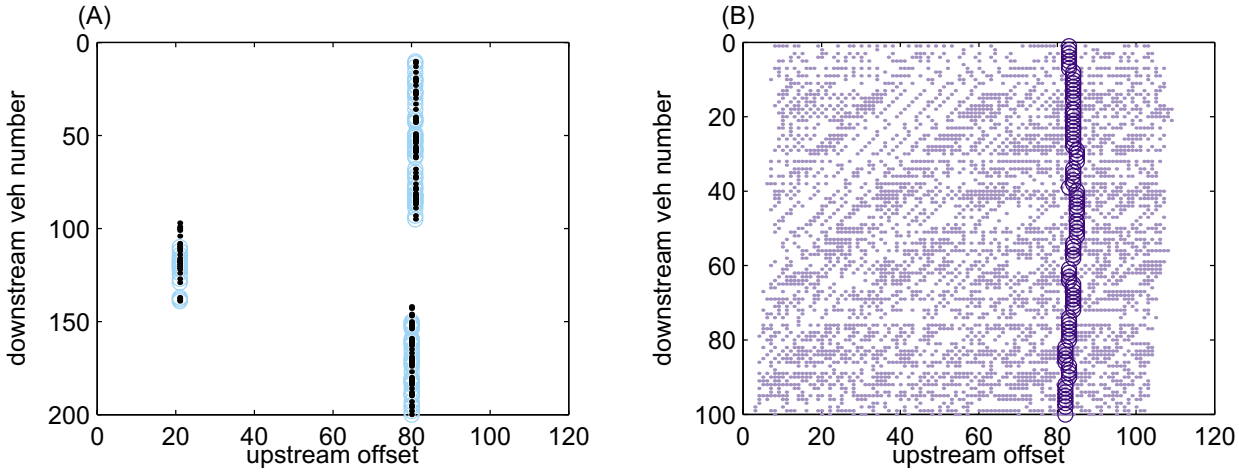

Figure 2-9 (A) Best match per row after one lane change maneuver (dark points) and five lane change maneuvers (light circles), (B) final matches from the data shown in Figure 2-3 (dark circles) and the original VMM (light points).

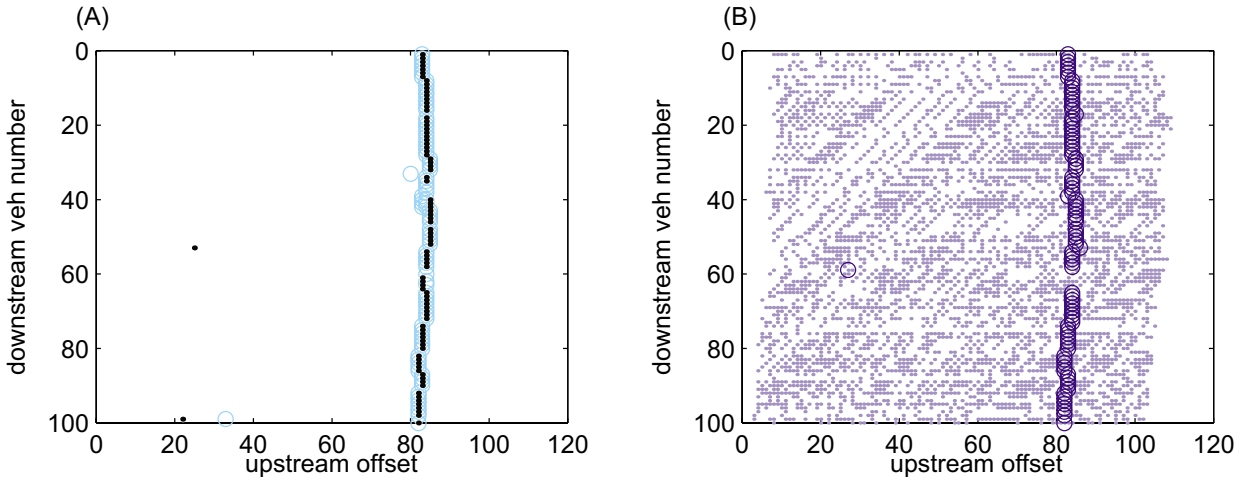

Figure 2-10 Resulting travel times from the matched vehicles (light X's) and ground truth travel times (dark line) for the first scenario, (A) Applying the Filter Test: 1206 final matches, (B) Applying the Cone Test: 1109 final matches, (C) Applying the Travel Time Test: 1182 final matches, (D) Applying the Multiple Lane Change Test: 1304 final matches (E) Combining the results from all four tests: 1267 final matches, (F) Applying all four tests and the final travel time filter: 1218 final matches.

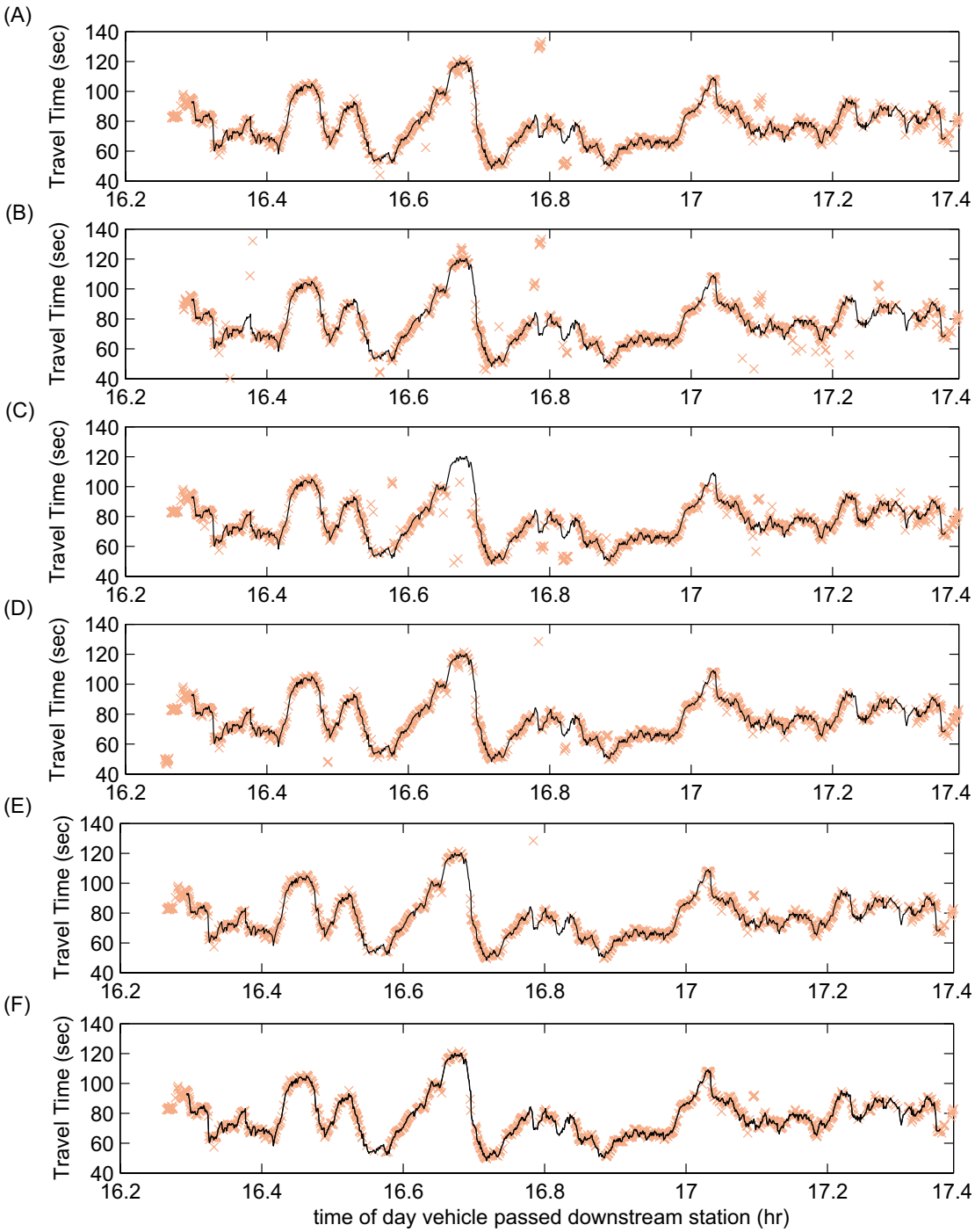

Figure 2-11 Resulting travel times from the matched vehicles (light X's) and ground truth travel times (dark circles) for the second scenario. (A) Lane 1 (inside, High Occupancy Vehicle lane), (B) Lane 2, (C) Lane 3, (D) Lane 4, (E) Lane 5 (outside lane).

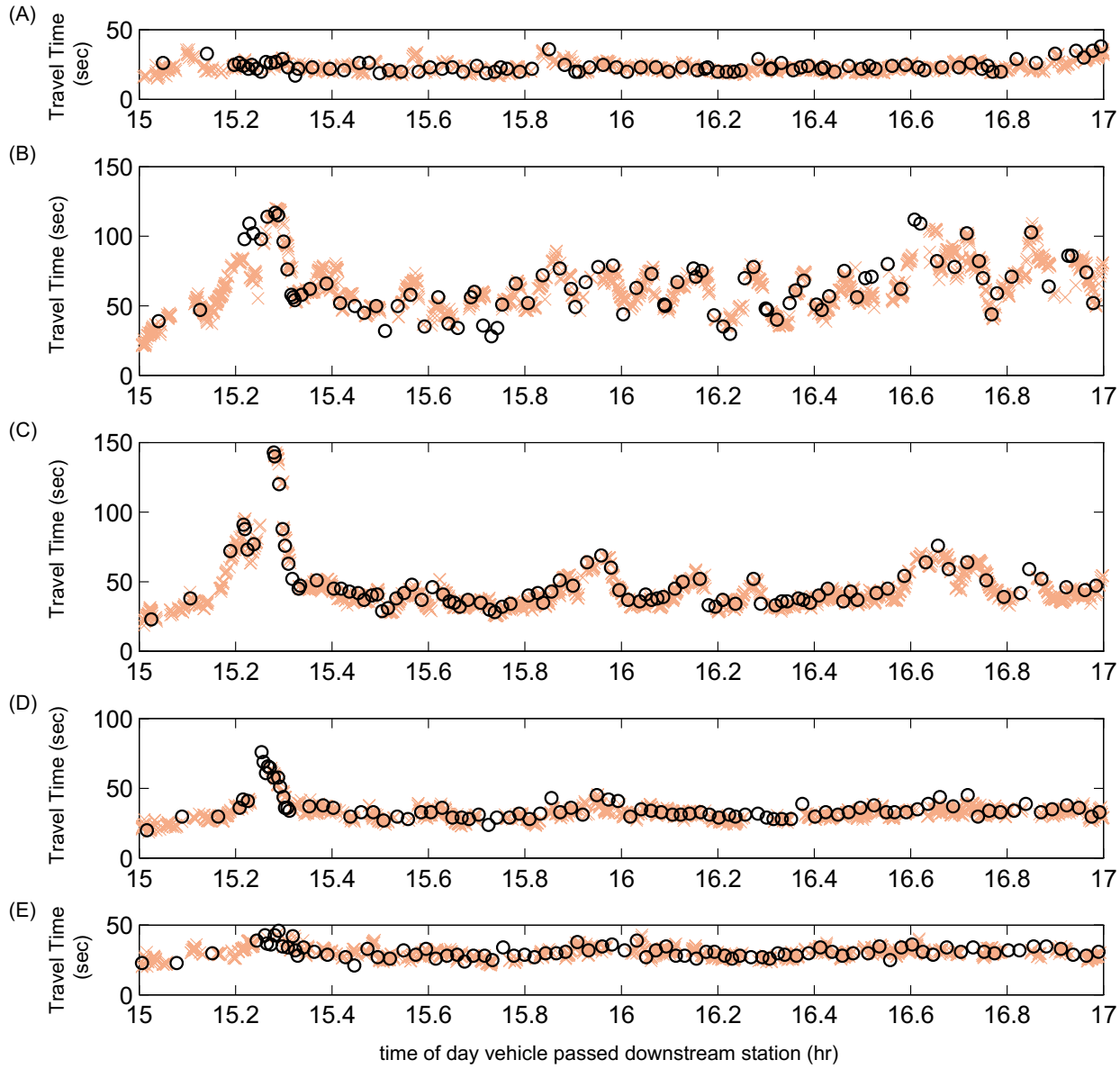

Table 2-1 Final results for the first scenario for each of the tests applied to a consecutive set of 1462 downstream vehicles, out of which 1269 vehicles passed both detectors and the remaining 193 vehicles entered the lane between the two stations (compare to matches found during period with ground truth).

			During period with ground truth			
		Total Final Matches From Entire Set	Final Matches	Correct Matches	Incorrect Matches	Average Absolute Percent Error in Travel Time for Final Matches
Before Final Filter	Filter	1206	1127	1054	73	5.60
	Cone	1109	1036	933	103	9.89
	Travel Time	1182	1099	1025	74	2.37
	Multiple Lane Changes	1304	1197	1111	86	6.59
	Combined Tests	1267	1180	1108	72	4.94
After Final Filter	Filter	1160	1082	1048	34	1.44
	Cone	1013	950	905	45	1.93
	Travel Time	1147	1068	1012	56	1.80
	Multiple Lane Changes	1231	1137	1102	35	1.44
	Combined Tests	1218	1132	1094	38	1.45
Ground Truth Matches			1269			

Table 2-2 Final results for the second scenario, percentage of passing vehicles matched from the *new* and *old algorithms*.

	Percentage of vehicles that were matched				
	Lane 1 (inside)	Lane 2	Lane 3	Lane 4	Lane 5 (outside)
New Algorithm	51.0%	54.7%	64.8%	44.7%	34.6%
Old Algorithm	38.5%	37.3%	39.3%	19.7%	8.9%

3 VEHICLE REIDENTIFICATION AND TRAVEL TIME MEASUREMENT ON FREEWAYS USING SINGLE LOOP DETECTORS- FROM FREE FLOW THROUGH THE ONSET OF CONGESTION[2]

3.1 Introduction

Traditional traffic surveillance strategies use loop detectors to calculate aggregate measures, such as flow and occupancy, at discrete locations on a freeway. Typically, these point measurements are assumed to be representative of extended links spanning detectors. This assumption is usually not valid when the facility becomes congested, e.g., when an incident occurs between two detector stations it can take several minutes before speeds drop at either of the stations.

The limitation of point data has spurred interest in vehicle reidentification techniques, which match the observations of the same vehicle at successive detector stations, e.g., Kuhne and Immes (1993), Huang and Russell (1997), Cui and Huang (1997), Balke et al. (1995). All of these earlier works require new detector hardware to extract detailed *vehicle signatures*. Often times, these advanced technologies are developed without consideration for the general goals of traffic surveillance, and as a result, an operating agency may risk investing in an expensive surveillance system to capture extraneous information. The systems also risk discarding useful information, e.g., in some cases, the tools collect link data but are not capable of measuring point data.

From an operations standpoint, the most important task of a surveillance system is determining reliably whether the facility is free flowing or congested. Conventional loop detectors meet this goal, but the response time to delays between detector stations can be excessive (Lin and Daganzo, 1997). Some of the advanced surveillance technologies promise to satisfy all of these tasks, but they have yet to see widespread deployment. In contrast to investing in new detector hardware, earlier work by our group developed a methodology to match vehicle measurements between conventional dual loop detector stations during free flow conditions (Coifman, *in press*). This Section extends the work to single loop detectors using the standard bivalent measurements. Key to the new approach is the ability to estimate vehicle lengths accurately at single loop detectors (Coifman et al., *in press*).

The algorithm identifies relatively distinct vehicles, i.e., long vehicles, at the downstream detector station and then for each of these vehicles it looks for a similar vehicle in the same lane at the upstream station within a time window of *reasonable* free flow travel times. Thus, if traffic is free

---

[2] B. Banerjee helped prepare this Section.

flowing over the link between detectors, this approach will usually find a match in the time window. If the freeway is congested, vehicles will be delayed and the true match for a vehicle will not be found in the time window. In the event a match is found the algorithm can also calculate that vehicle's travel time by taking the difference in the vehicle's arrival time at the two locations. In other words, the algorithm is capable of reporting free flow travel times or that "traffic is not free flowing".

3.2 Determining if Traffic is Free Flowing

All vehicles that traverse a link between two detector stations must, by definition, pass both stations. For these vehicles, every downstream observation should have a corresponding upstream observation and the time between these two observations is simply that vehicle's link travel time. These travel times are not known a-priori; however, if the vehicle travels at free flow velocities over the entire link, the travel time must fall within a known range of free flow travel times. This concept is illustrated in Figure 3-1. For the present study, the free flow travel time range is defined as follows:

$$ttR_0 = \left[\frac{\text{distance}}{\max(w+16,88)}, \quad \frac{\text{distance}}{\max(w-16,72)} \right] \tag{3-1}$$

where

ttR_0 = the range of feasible free flow travel times [h],
w = local velocity estimate at the downstream detector station, as defined below, [km/h],
distance = the known distance between detector stations [km].

To keep the search window as short as possible, while also being able to accept a wide range of free flow velocities, Equation 3-1 will select the assumed velocity range to be [72,88] km/h if $w<72$ km/h and $w\pm16$ km/h if $w>88$ km/h. These constants were determined empirically, but they have proven robust when applied to many different freeway links.

Chang and Kao (1991) suggest that at most locations, lane change maneuvers are relatively infrequent during free flow conditions and the experimental results in subsequent subsections support this observation. So a free flow vehicle observed at the downstream station will usually have a corresponding observation at the upstream station in the same lane, in the time window bound by ttR_0. Congestion will disrupt this relationship, both because the travel time will increase

beyond the free flow travel time range and because there may be an increase in lane change maneuvers, particularly if one or more lanes are blocked.

3.3 Vehicle Measurements

For a given downstream vehicle, many upstream vehicles may be observed in the corresponding time range. Estimated vehicle length, as defined in Coifman et al. (*in press*) and summarized in this subsection, is used to differentiate between vehicles. For each vehicle at each detector, the algorithm estimates velocity, $\hat{v}$, with the following equation,

$$\hat{v} = \frac{L}{median(on)} \tag{3-2}$$

where the on-time, *on*, is simply the amount of time that the detector is occupied by the vehicle. The constant, *L*, represents the assumed median vehicle length and the median on-time comes from 19 consecutive vehicle measurements centered on the subject vehicle. If one assumes that all of the vehicles in a sample are traveling near the median velocity, one can use Equation 3-2 in conjunction with measured *on* to estimate individual vehicle lengths, $\hat{l}$, with the following equation,

$$\hat{l} = \hat{v} \cdot on = \frac{L \cdot on}{median(on)} \tag{3-3}$$

The length range, *LR*, is defined as,

$$LR = [\text{min length est}, \quad \text{max length est}] = [0.995, \quad 1.045] \cdot \hat{l} \tag{3-4}$$

and the measurement uncertainty is defined as the difference between the maximum and minimum length estimates. Of course the occasional measurement error will result in an erroneous *LR* for that vehicle, but the methodology was specifically designed to accommodate these errors.

Next, the algorithm compares length estimates between detector stations. If the length range for a downstream observation overlaps that of an upstream observation, then the two observations may have come from the same vehicle. Otherwise the result of the pair-wise comparison can be dismissed as an unlikely match because even allowing for the measurement uncertainty the two ranges do not intersect.

Most observations are passenger vehicles and their lengths fall in a small range, e.g., roughly 80 percent of the observations fall between 5 m and 7 m for the data used in this study. It is difficult to

differentiate between these short vehicles. In contrast, some length observations are as long as 24 m. The large range of feasible lengths and the lower frequency of observations for the long vehicles make it possible to differentiate between them.

3.4 Algorithm Implementation

Using an example to illustrate the algorithm implementation, we consider a 0.55 km freeway segment from the Berkeley Highway Laboratory (Coifman et al., 2000). This facility is equipped with eight dual loop detector stations. We use a single loop at two neighboring stations to demonstrate the methodology and then verify the results using the corresponding dual loop data (Coifman, *in press*).

To eliminate the common vehicles, all downstream vehicles shorter than 7 m are ignored. Whenever a long vehicle passes the downstream loop detector the algorithm searches a fixed time earlier, bounded by Equation 3-1, for any upstream vehicles in the same lane whose length range, as defined by Equation 3-4, intersects the downstream vehicle's length range. If an intersection is found, the corresponding upstream vehicle is considered a possible match and the downstream vehicle is assigned a value of one. If more than one intersection is found within the time window, then arbitrarily, the most recent of these upstream observations is considered the possible match. Otherwise, the downstream vehicle does not have an identifiable free flow match in the lane and that vehicle is assigned a value of zero.

Obviously, a free flow vehicle will not have a match in the same lane if the vehicle changed lanes, entered the freeway between detectors, or because of a misdetection at one of the stations. On the other hand, a delayed vehicle should not have a match (Figure 3-1B), but another vehicle of similar length may have passed within the time window. To eliminate most of these false positives, possible matches are suppressed in subsequent stages of the algorithm if there are fewer than two possible matches in the preceding six trials (including any suppressed matches). Next, we take a moving average of the 10 most recent outcomes (including the current outcome). Figure 3-2A shows this moving average for just over 20 hours of data from the single loop detectors. For reference, Figure 3-2B shows the corresponding averages using the dual loop data. Applying a threshold to these data, Figure 3-3 shows the travel times for all of the long vehicles that had a possible match and a moving average over 0.2 in Figure 3-2.

The goal of the algorithm is to detect when travel times start to increase. The onset of congestion is characterized by a dramatic increase in link travel times. When this occurs, the true travel times will not fall within the range specified by Equation 3-1. Notice that the single loop algorithm found few

fast matches between 6 and 10 hours, which corresponds to the same time range when the dual loop algorithm found few matches. The lack of matches in this case is due to the fact that a downstream queue overruns the segment. Although the measured travel times in Figure 3-3 are useful for traffic surveillance, the true diagnostic power of the method comes from the moving average in Figure 3-2. The free flow periods are characterized by high average values and congested periods by low average values.

Looking closer at the travel times in Figure 3-3, there is a transition period as the queue first overruns the downstream detector and eventually covers the entire link. This transition is characterized by increasing travel times, as can be seen just after 6 hours. In an attempt to capture the increasing delays during the transition, one can define additional travel time ranges (*ttR's*), each one with a slower link velocity than its predecessor and use the same methodology outlined above for these new *ttR's*. Using dual loop data, earlier work has shown that as a queue grows across the link, the true travel times will pass from one *ttR* to the next (Coifman, *in press*). The onset of congestion can then be identified as the instant the fastest *ttR*, i.e.ttR_0, ceases to contain highest moving average among all of the *ttR's*.

3.5 Limitations at Single Loop Detectors

The use of Equation 3-3 requires the assumption that most vehicles in the moving median have a length close to *L*. Close examination of Figure 3-2A reveals at least two cases near 14 hours where this assumption breaks down and the moving average drops even though traffic is free flowing. Figure 3-4A shows a detail of this moving average. Figure 3-4B shows the corresponding measured and estimated lengths at the downstream detector. Notice that many successive long vehicles passed, resulting in a low velocity estimate, shown in Figure 3-4C, and thus, a low length estimate. This error prevented the algorithm from finding matches for the long vehicles and impacted the moving average for several following vehicles because even after the velocity estimate recovered, several possible matches were suppressed due to the low frequency earlier matches. Fortunately, these velocity errors can be identified using a slightly more sophisticated estimation process, e.g., using occupancy to help identify free flow periods at the detector and set the velocity estimate accordingly (Coifman, 2001).

3.6 Conclusions

This Section has developed a new traffic surveillance strategy using existing single loop detectors. Rather than reporting local conditions at the detectors, the strategy identifies periods when the link between two detector stations becomes congested. Unlike most surveillance strategies that attempt

to match vehicle measurements between detector stations, this work is compatible with the existing detector infrastructure.

To place the work in context, the algorithm has a lower reidentification rate than the other methods that require new hardware, but perhaps the higher rate is not necessary. One could view the algorithm as a low cost means to investigate the benefits of vehicle reidentification and travel time data before investing in a new surveillance system. In any event, the algorithm is intended to augment, rather than supplant, conventional point detector measurements. By combining point detector data with the new link data, it should be possible to identify transients in either data set and improve performance beyond what would be possible with just one of these data sets.

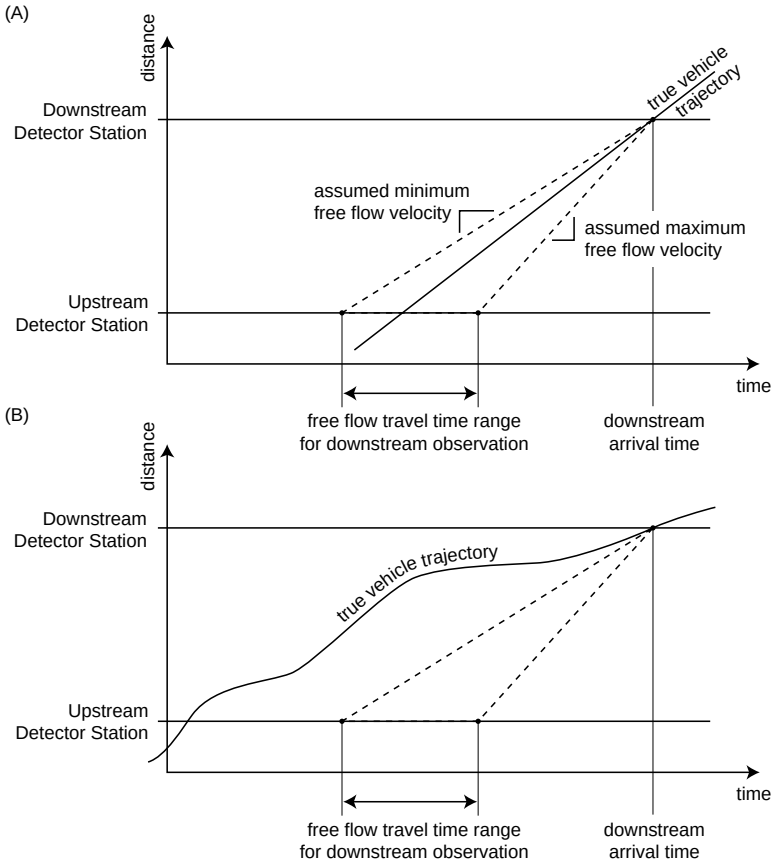

Figure 3-1 One vehicle traversing an extended link between two detector stations, illustrating the free flow travel time range. (A) The vehicle travels at a free flow velocity and it was observed at the upstream station during the time range; (B) the vehicle traveled slower than the minimum free flow velocity and it passed the upstream station before the start of the time range.

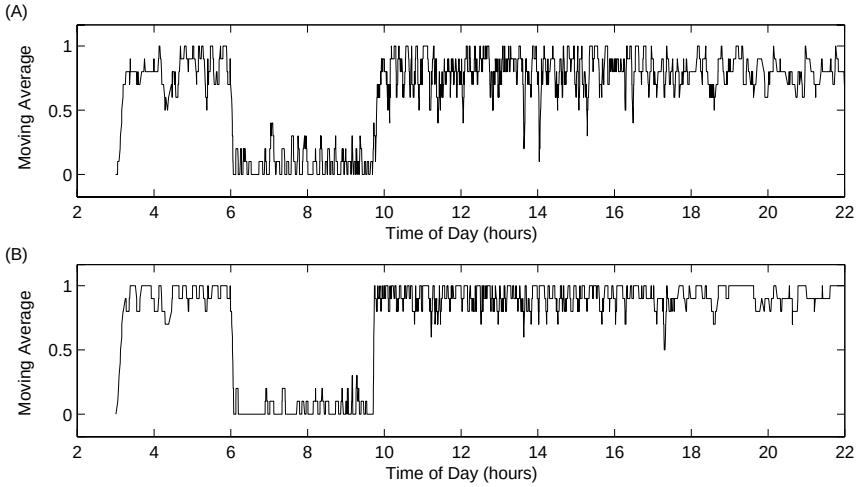

Figure 3-2 Each pair-wise test is assigned a value of 1 if a match is found and 0 otherwise. This figure shows the moving average using (A) single loop data (B) dual loop data.

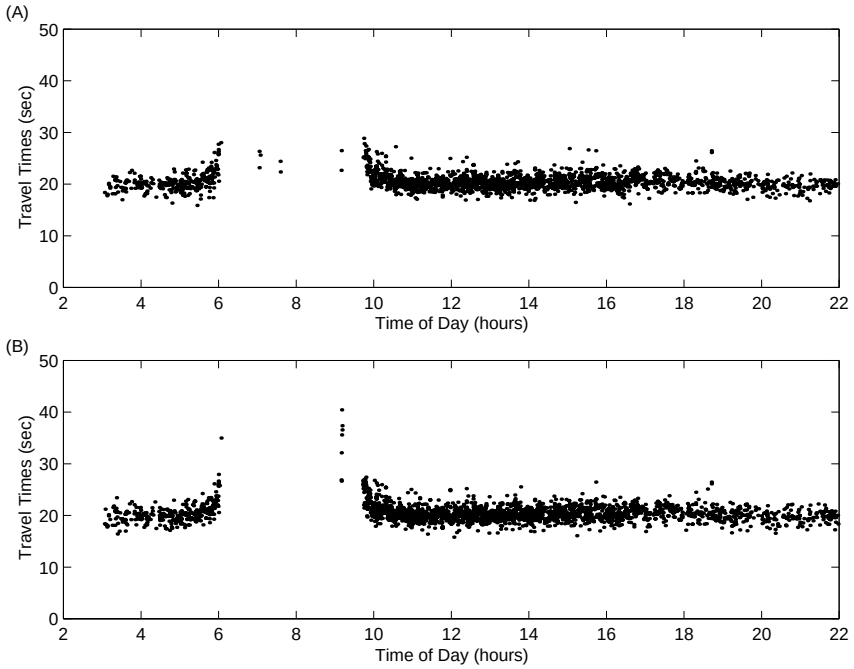

Figure 3-3 The resulting travel times for the matches from Figure 3-2 (A) single loop data (B) dual loop data.

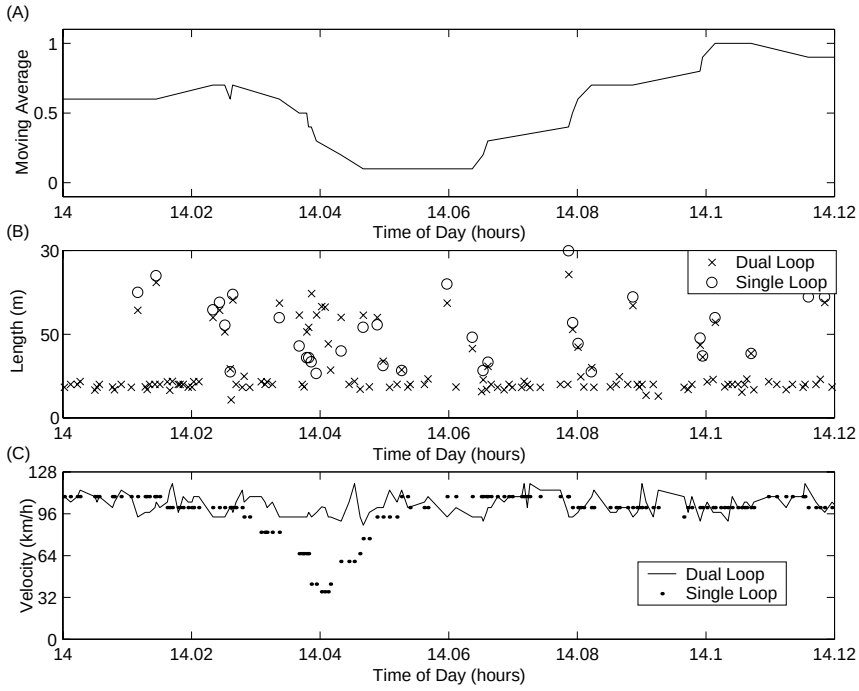

Figure 3-4 Detail showing (A) a dip in the single loop detector moving average at 14.04 hr, during free flow conditions. (B) The measured and estimated lengths, note several long vehicles pass in a group resulting in (C) a drop in the estimated velocity and thus, a drop in the estimated lengths.

4 ESTIMATING DENSITY AND THE NUMBER OF LANE CHANGE MANEUVERS IN A FREEWAY SEGMENT

4.1 Introduction

Virtually all traffic flow models are based on the relationships between flow, q, density, k, and velocity (space mean speed), v. This fact is due to the spatial and temporal nature of traffic flow and has been reflected all the way back to the seminal works on traffic flow theory, e.g., Greenshields (1935), Lighthill and Whitham (1955) and Richards (1956). One can easily measure q and v at a point in space with conventional traffic detectors, but k is more difficult to measure. Although in theory, density could be measured between detector stations using simple input-output models, vehicle detectors are imperfect and detector drift precludes such simple measurement. Most traffic flow theory has been developed using point measurements and in some cases, resource-intensive data collection efforts to capture spatial information. The latter were typically short-term studies, often consisting only of a few minutes or a few hours of data, and were usually based on photogrammetric tools dating back to Greenshields (1934). In addition to the difficulties of capturing simple spatial measurements such as k, it has long been recognized that lane change maneuvers can influence the relationships underlying traffic flow theory or even disrupt the relationships if lane change maneuvers are not accounted for. While density can be measured from a single image, quantifying lane change maneuvers requires both spatial and temporal coverage.

Considerable efforts have been made to estimate and model density: Gazis and Knapp (1971), Nahi and Trivedi (1973), Gazis and Szeto (1974); lane changing frequency: Worrall and Bullen (1970), Worrall, Bullen and Gur (1970), Phal (1972), Munjal and Hsu (1973), Gang and Kao (1991); as well as the combination of density and lane changing behavior: Chang and Gazis (1975), Sheu (1999). The density models must accept a large uncertainty range due to conventional operation of vehicle detectors, while many of the lane change models assume accurate measurement of density. All of the models are limited by the small amount of available spatial data for validation. For example, in most cases lane changing was modeled as a function of flow, but it is likely that excluded factors such as location, time of day, and vehicle mix are significant.

Recent advances in traffic surveillance could solve this data deficiency. Video image processing and vehicle tracking tools may soon be accurate enough to extract density and lane changes within a limited field of view. However, occlusion and oblique viewing angles limit the distance that one camera can be used to automatically extract such data and a vehicle traveling at free flow speeds will likely be out of (trackable) view within a few seconds.

In the mean time, Reijmers (1979) presented new vehicle detection hardware that is compatible with existing loop detectors and is capable of extracting detailed magnetic vehicle signatures. Kuhne and Immes (1993) and others have since used these signatures to match a vehicle's measurements between one location and another, so-called *vehicle reidentification*. By matching almost every vehicle, these new loop based systems could provide direct measurement of true density and lane change frequency. So far, the new detectors have seen limited deployment because they require additional hardware and considerably higher communication bandwidth compared to conventional loop detectors.

Recent work by our group has produced an alternative to the hardware intensive vehicle reidentification tools. Our approach uses the existing vehicle detection hardware and communication infrastructure. Unlike the detailed magnetic signatures, the approach uses the standard bivalent loop detector output to measure effective vehicle lengths at dual loop detectors. These vehicle measurements are assigned sequential arrival numbers in each lane at each detector station, denoted $N_u(t)$ and $N_d(t)$ for the upstream and downstream stations, respectively. Two complementary algorithms use these length measurements, arrival numbers and arrival times to reidentify vehicles between detector stations. The first algorithm attempts to find a match for every vehicle during congestion (Coifman and Cassidy, in press), while the second only attempts to match unique vehicles during free flow conditions (Coifman, in press). The operating regions of the two algorithms overlap, allowing for uninterrupted vehicle reidentification. The algorithms are not able to match every vehicle under the limited resolution of the loop detector length measurements. Experimental results found that the congestion algorithm can match up to 75 percent of the passing vehicles while the free flow algorithm can match up to seven percent. These reidentification rates are sufficient for travel time measurement (Van Aerde et al., 1993, Holdener and Turner, 1996) and the algorithms have been running continuously in the Berkeley Highway Laboratory (BHL) for several years[3] on Interstate 80, north of Oakland, California (Coifman, Lyddy and Skabardonis, 2000). This Section will show how the resulting matches can be used to estimate density in a freeway lane between detector stations and measure lane inflow, the difference between the number of lane change maneuvers that enter and the number that exit the lane.

These new measurements have many potential applications. First, they could help verify and calibrate earlier density and lane changing models, allowing data collection over an extended period at a large number of locations. Second, the new traffic parameters should improve incident detection and assessment, e.g., identifying increased lane change maneuvers that deviate from

[3] The real time system can be viewed at: http://www.its.berkeley.edu/projects/freewaydata.

historical lane inflow patterns. Third, lane inflow can lead to better detector diagnostics because the net inflow summed over all lanes should be zero if there are detectors at all entrances and exits. Similarly, as will be shown in this Section, lane inflow can be used to estimate ramp flow using only the mainline detectors. This point is important because, depending on the ramp geometry, drivers may ignore striping and make it difficult to place ramp detectors to ensure accurate detection of all vehicles. The remainder of this Section presents the density estimation and lane inflow measurement techniques given a vehicle reidentification methodology that only matches a portion of the passing vehicles.

4.2 Density Estimation

The vehicle reidentification algorithms developed by our group provide data on a small percentage of the vehicles passing on the segment between detector stations. Figure 4-1 shows an example of the matches from Coifman and Cassidy (in press) for 100 consecutive vehicles at the downstream detector in one lane on an 1,800 ft freeway link in the BHL. The downstream vehicle number, N_d, is shown on the horizontal axis and offset between the vehicle numbers, N_d-N_u, for each match on the vertical axis. Notice that approximately 30 percent of the vehicles do not have matches in this figure. Although the reidentification rate from the two vehicle reidentification algorithms can be significantly lower then shown in this example, the measurements capture valuable spatial information about the traffic conditions between the stations. Although the algorithms may not match every vehicle, assuming few detector errors, conventional loop detector data contain information on the entire vehicle population passing a single point. Combining the point data with the matched vehicle data, it is possible to estimate link density at two instants for each reidentified vehicle. Consider the case where downstream vehicle measurement $N_d(t_2)$ is matched to upstream vehicle measurement $N_u(t_1)$. The travel time for this vehicle is simply t_2-t_1. If no vehicles change lanes, then all vehicles that passed the upstream station while the matched vehicle traversed the link must still be in the lane at time t_2 and no other vehicles will be in the lane. Similarly, all vehicles that were in the lane at time t_1 will have passed the downstream detector by t_2 and no other vehicles will have exited during the period that the matched vehicle traversed the link. Of course the assumption that no vehicles change lanes is unreasonable. Relaxing the assumption such that most vehicles do not change lanes leads to the following two estimates of lane density each time a vehicle is matched between the two stations:

$$\hat{k}_u(t_2) = \frac{N_u(t_2) - N_u(t_1)}{\text{distance}} \tag{4-1}$$

$$\hat{k}_d(t_1) = \frac{N_d(t_2) - N_d(t_1)}{\text{distance}} \tag{4-2}$$

Where $\hat{k}_u$ and $\hat{k}_d$ are based on the upstream and downstream arrivals, respectively, as illustrated in Figure 4-2.

The points in Figure 4-3A-B show the resulting density estimates after applying Equations 4-1 and 4-2 to just over an hour of dual loop data from the same 1,800 ft freeway segment used in Figure 4-1. For comparison sake, the density estimates from the upstream station are shifted in time to the clock at the downstream detector station using the measured travel times. In this case, measured speeds at the dual loop detectors were on the order of 20 mph and approximately 1,400 vehicles passed the downstream detector during the sample period. Concurrent video data were collected at both stations and all vehicles in the lane were manually matched during the same time period. The resulting density estimates from the manually matched vehicles are shown with solid lines in Figure 4-3A-B. Figure 4-3C compares the two manual density estimates. If there were no lane change maneuvers the two density curves should fall on top of one another, but they are within seven percent of one another on average, with a few transients out to 30 percent. These differences are due to the fact that some vehicles do change lanes and the comparison in Figure 4-3C illustrates the benefit of making the two estimates. Simply put, it is not the increased sampling frequency, since $\hat{k}_d(t_1)$ cannot be made until after the matched vehicle leaves the link at t_2, rather, it is the redundancy between the two independent estimates that can be used to highlight periods in which the accuracy of the estimates may be reduced due to lane change maneuvers.

The next subsection will address these lane change maneuvers. But before proceeding, it is worth noting that given a sufficiently accurate travel time estimation methodology, these equations also apply in cases without vehicle reidentification. For example, Coifman (2002) presents an algorithm to estimate travel time using data from a single detector station and one could apply these equations with the modification that t_1 is estimated in Equation 4-1 and t_2 is estimated in Equation 4-2.

4.3 Lane inflow Estimation

Assuming few detector errors, most of the drift in $N_d(t_2)$-$N_u(t_1)$ for the set of matched vehicles will be due to the lane inflow. The lane inflow can be measured even with a low frequency of vehicle reidentification. The two vehicle reidentification algorithms mentioned previously only match vehicles when they can, but more importantly, these matches are made relative to the local arrival numbers at each detector station, N_u and N_d. The lane inflow is simply the change in offset and the

lane flux is defined as the time derivative of the inflow. Both values can be calculated whenever a new match is found. Consider Figure 4-1, no matches were found for downstream vehicles numbered 55 to 78. The difference in the upstream offset before and after the gap indicates a net inflow of -4 vehicles, i.e., 4 vehicles left the lane during the gap of 24 downstream vehicles without matches. Although not shown on the plot, the times each vehicle passed the detectors were recorded.

Using data from the I-880 Field Experiment (Skabardonis et al., 1996), both vehicle reidentification algorithms were applied independently to each lane of a five lane freeway segment south of Oakland, California. The segment is 1,500 ft long with an on-ramp near the upstream detector station (inset, Figure 4-4A). Three hours of data were used and no attempt was made to explicitly account for lane change maneuvers or entering vehicles while matching vehicles. The number of vehicles and percentage that were matched for this example are presented in Table 4-1. For each match in a given lane, the upstream offset versus downstream arrival time is shown in Figure 4-4A. The slope of each curve is the lane flux, quantifying the net number of vehicles that enter (positive slope) or exit (negative slope) the given lane per unit time, over the distance that spans the two stations. Lane 5 (the outside lane) had a net inflow of 856 vehicles and lane 4 had a net inflow of 405 vehicles during the three hour period. The remaining lanes saw a smaller net inflow during the same period. Summing the inflow across all five lanes yields the gray line in Figure 4-4B and a net inflow of 1,360 vehicles. During the same period, 1,384 vehicles passed a detector on the on-ramp and these arrivals are shown with a black line in Figure 4-4B, while the difference between the two curves is shown in Figure 4-4C.

Although the vehicle reidentification algorithms were applied to each of the mainline lanes independently -- ignoring both the other lanes and the presence of the ramp -- and only 11 percent of the vehicles were matched, the net lane inflow and on-ramp flow are within two percent of one another. Figure 4-4D shows the time series velocity for reference and it is clear that the matches come from free flow conditions prior to 8:00 and congested conditions thereafter.

Returning to the BHL for a larger example,[4] the process is repeated over 24 hours on a five lane, 1,800 ft long segment without ramps. Once more, the reidentification algorithms were applied to each lane independently. The number of vehicles and percentage that were matched for this example are presented in Table 4-2. Figure 4-5A shows the time series evolution of the inflow for all of the lanes on the segment and the inset shows a schematic of the location. The lane changing patterns are due to the split of I-80, I-580 and I-880 less than two miles downstream of the study

segment. Lane 1 is a high occupancy vehicle lane and on most days, lane 2 usually experiences the heaviest downstream congestion due to traffic backed up from the left-hand branch of the diverge. This plot shows three transient periods of high lane flux in lanes 2 and 5, as enumerated in Table 4-3 and normalized for distance. Obviously, vehicles can not move directly between non-adjacent lanes, so these data indicate movement through all of the intervening lanes. The additional lane change maneuvers in lanes 3 and 4 are roughly balanced, i.e., after removing the long-term trend, one vehicle leaves lane 4 between the stations for each vehicle that enters the lane. This example illustrates the fact that the net inflow differs from the total number of lane change maneuvers. For reference, Figure 4-5B-C show the time series velocity at the upstream and downstream stations, respectively. As shown with dashed lines on these plots, the periods of high lane flux listed in Table 4-3 correspond to mixed traffic conditions on the link: free flow at the upstream station and congested at the downstream station. Apparently, when the tail of the queue is within the link, drivers exhibit different lane changing patterns. Quantifying this behavior will be the subject of further research.

Summing the inflow across all five lanes yields the curve in Figure 4-5D. Simply employing vehicle conservation, one would expect that the total inflow should be constant since there are no ramps in the link. Considering the fact that over 100,000 vehicles pass during the day, indeed the total inflow is nearly constant. Most of the drift in this curve is likely due to infrequent detection errors. However, there are two distinct periods in which the drift can be explained readily. First, at 9:35 a sharp spike is evident and is due to a brief error in the vehicle reidentification algorithm applied to lane 4. Then, a broader spike is evident for approximately half an hour, centered on 10:15. This event is due to an extended period without any matched vehicles in lane 2 coincident with the upstream detector returning to free flow conditions, as shown in Figure 4-5B. As discussed in Coifman (in press), the free flow vehicle reidentification algorithm can continue matching vehicles after the onset of congestion and into the range of the congestion algorithm. However, once a link becomes completely congested, the free flow algorithm does not resume matching vehicles until the entire link returns to free flow conditions. So as seen here, when a queue recedes over a link, travel times may leave the effective range of the congestion algorithm before they return to the range of the free flow algorithm and lead to a brief period without any matches from either algorithm. In any event, the broader spike is simply due to a lack of information from one of the lanes and does not represent an inflow estimation error.

---

[4] Unlike the I-880 Field Experiment, the BHL provides 24 hour a day coverage but lacks functional ramp detectors.

4.4 Conclusions

Although this Section is based on the basic principle of conservation of vehicles, it is the measured travel time that allows for density estimation and upstream offset that allows for lane flux and inflow measurement. The Section has shown that it is possible to capture the net effect of vehicle maneuvers in space using loop detectors. The work does not need a high frequency of matches, just accurate ones.

There are many applications for the new measurements, including real time incident detection and off line correlation between accident frequency and lane flux. The measures can also be used to verify the performance of detectors, any unexplained drift in inflow would likely be due to faulty detectors. The reader should be cautioned though, the fundamental equation, q=kv, does not hold unless care is taken to estimate q and k over the same region of the time-space plane, e.g., Edie (1963). Finally, although the methodology was demonstrated using loop detectors, it is potentially applicable to other detector technologies as well.

Table 4-1 Vehicle statistics for the three hour long I-880 lane inflow example in Figure 4-4.

	lane 1	lane 2	lane 3	lane 4	lane 5	total
Number of vehicles	2,052	5,593	4,298	4,210	3,885	20,038
Number of matched vehicles	203	439	611	554	342	2,149
Percent of vehicles matched	9.9	7.9	14.2	13.2	8.8	10.7
Net inflow	55	18	26	405	856	1,360
Inflow as percent of flow	2.7	0.3	0.6	9.6	22.0	6.8

Table 4-2 Vehicle statistics for the 24 hour long I-80 lane inflow example in Figure 4-5.

	lane 1	lane 2	lane 3	lane 4	lane 5	total
Number of vehicles	16,256	27,268	23,312	24,596	25,173	116,605
Number of matched vehicles	2,968	3,904	5,136	4,496	4,854	21,358
Percent of vehicles matched	18.3	14.3	22.0	18.3	19.3	18.3
Net inflow	584	-891	-979	-415	1,708	7
Inflow as percent of flow	3.6	-3.3	-4.2	-1.7	6.8	0.0

Table 4-3 Transient periods of high lane inflow in lanes 2 and 5 from Figure 4-5.

	Lane 2			Lane 5		
Approximate time of day (hr)	inflow (veh)	duration (hr)	lane flux per mile (veh/hr/mi)	inflow (veh)	duration (hr)	lane flux per mile (veh/hr/mi)
10:00	-170	0.6	-830	100	0.2	1,467
15:00	-240	0.8	-880	250	0.8	917
17:20	-130	0.5	-762	150	0.4	1,100

Figure 4-1, A sample showing the downstream vehicle number and offset for reidentified vehicles.

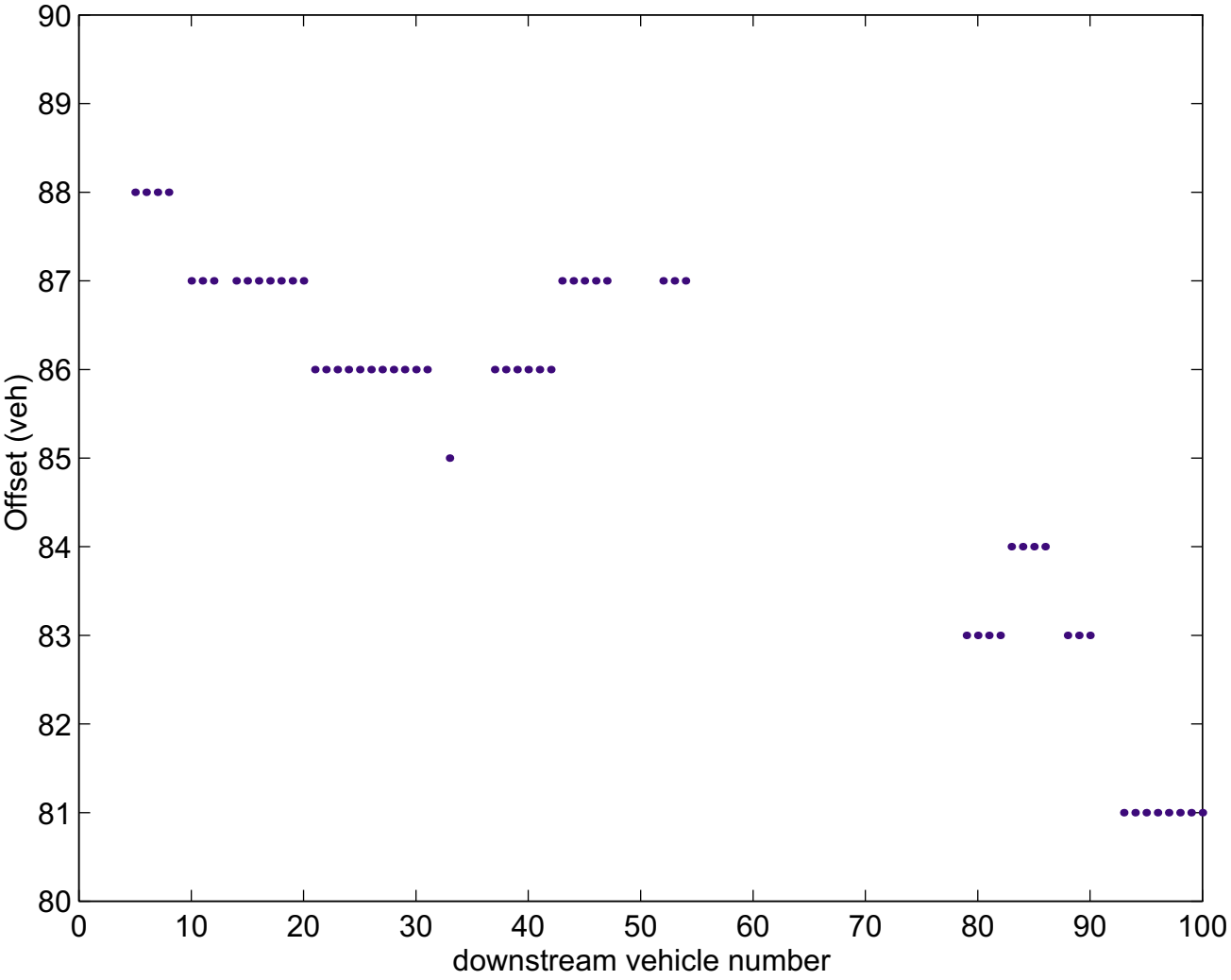

Figure 4-2, An example illustrating the two density estimates that are available after reidentifying a vehicle.

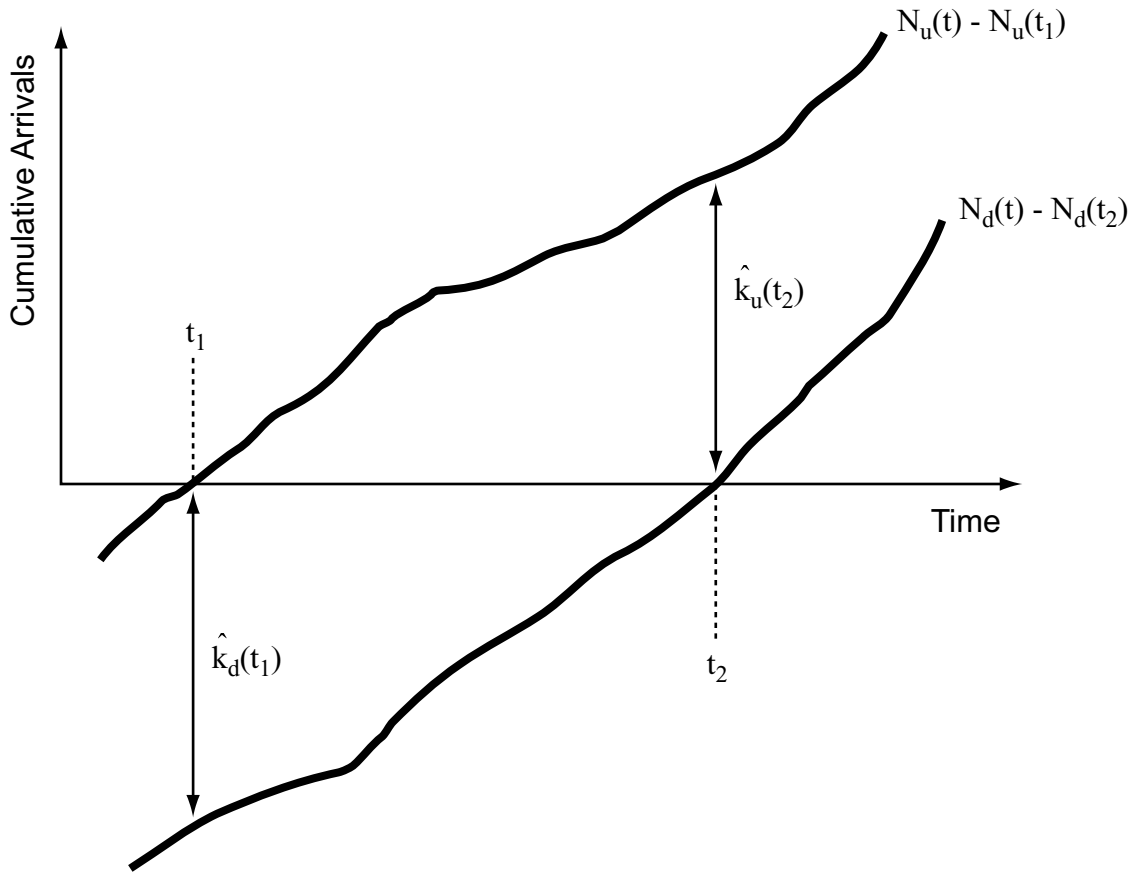

Figure 4-3, Density estimated from automated vehicle reidentification compared against those from manual reidentification (A) using upstream arrivals, (B) using downstream arrivals, (C) comparing upstream and downstream manual estimates.

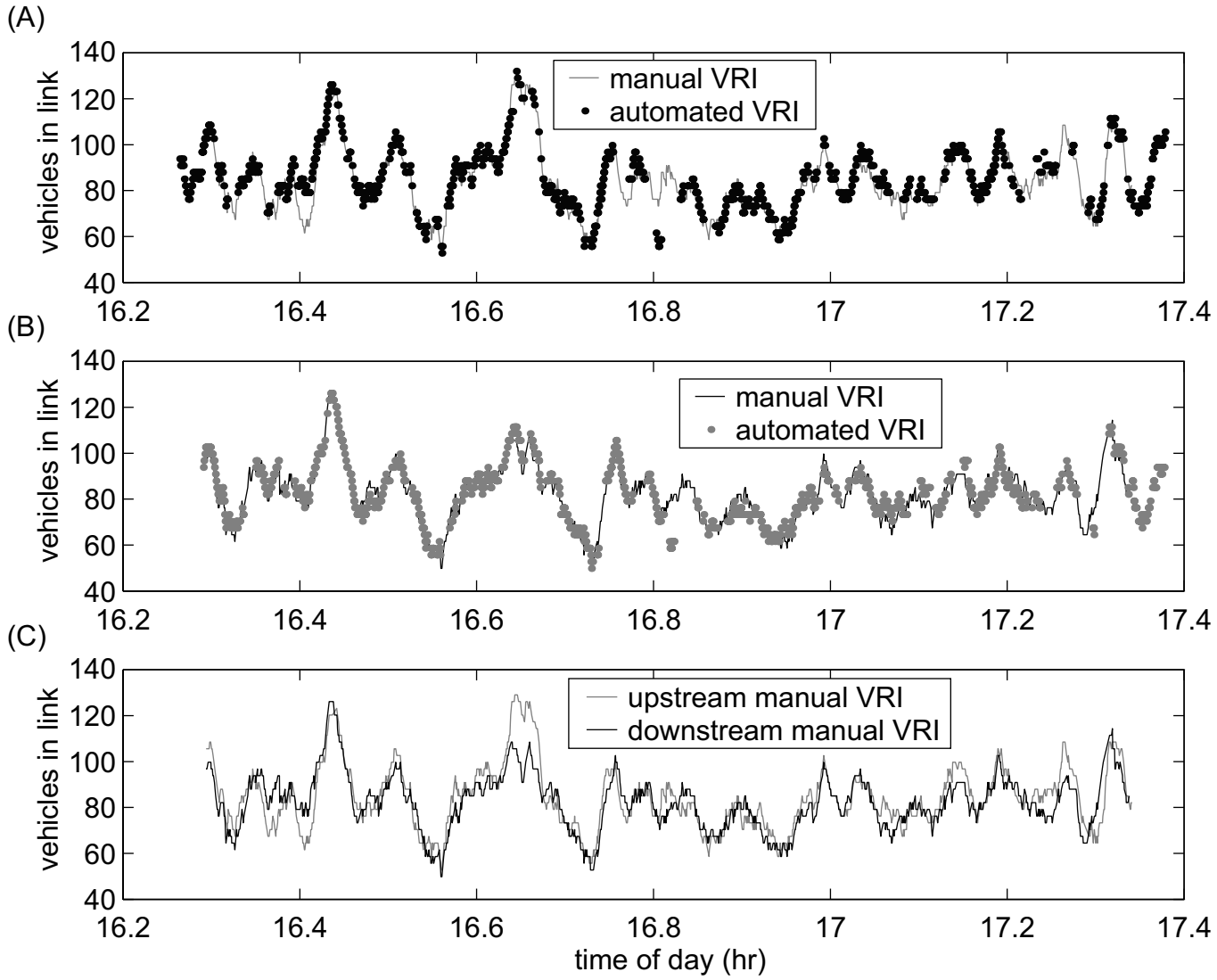

Figure 4-4, (A) Estimated lane inflow between two detector stations (inset) 1500 ft apart, (B) comparing the net lane inflow across all lanes to on-ramp arrivals, (C) difference between curves in part B, (D) 30 sec average velocity by lane during study period.

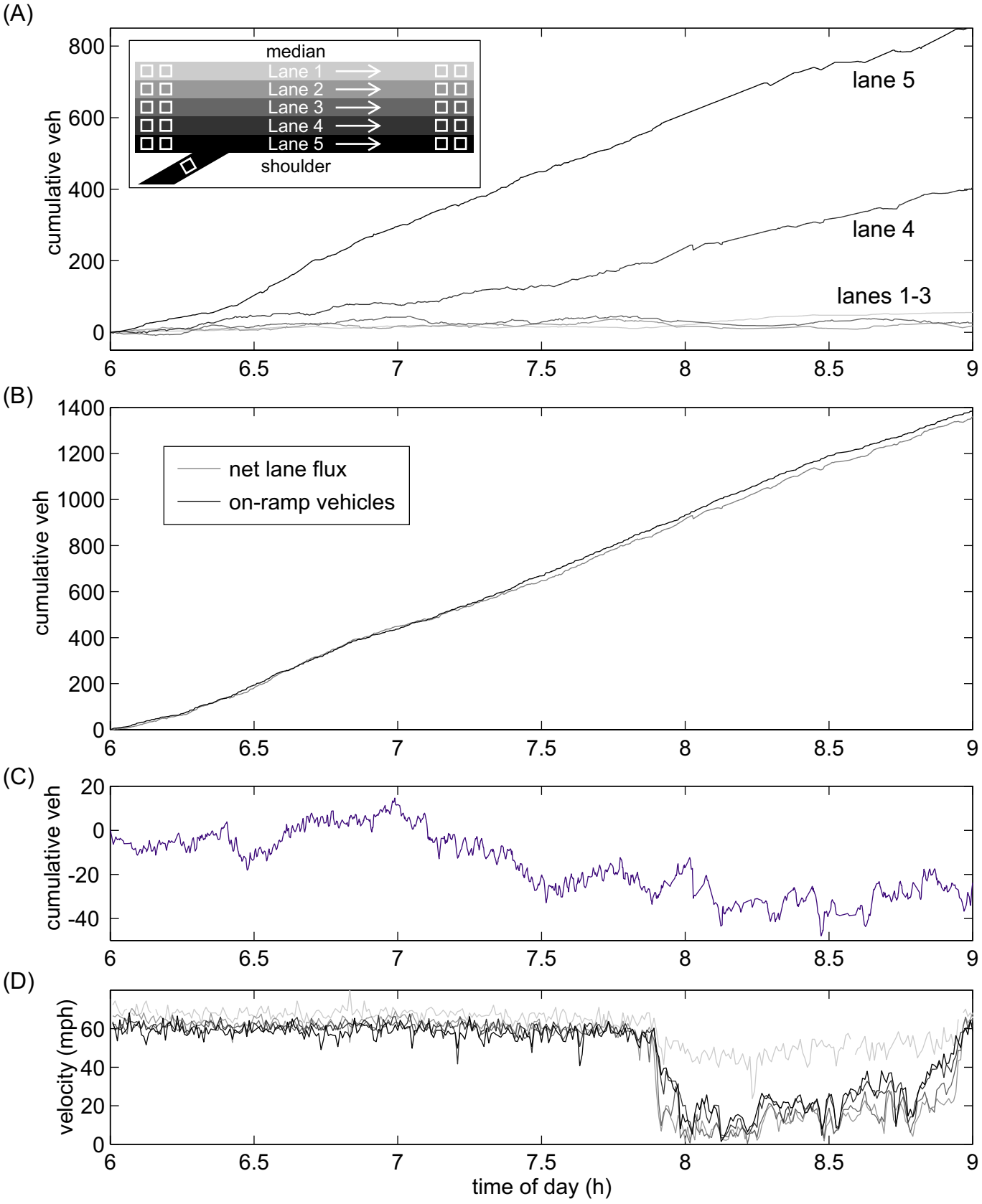

Figure 4-5, (A) Estimated lane inflow between two detector stations (inset) 1800 ft apart during 24 hrs, (B) five min average velocity by upstream lane, (C) five min average velocity by downstream lane, (D) change in net lane inflow across all lanes during the day.

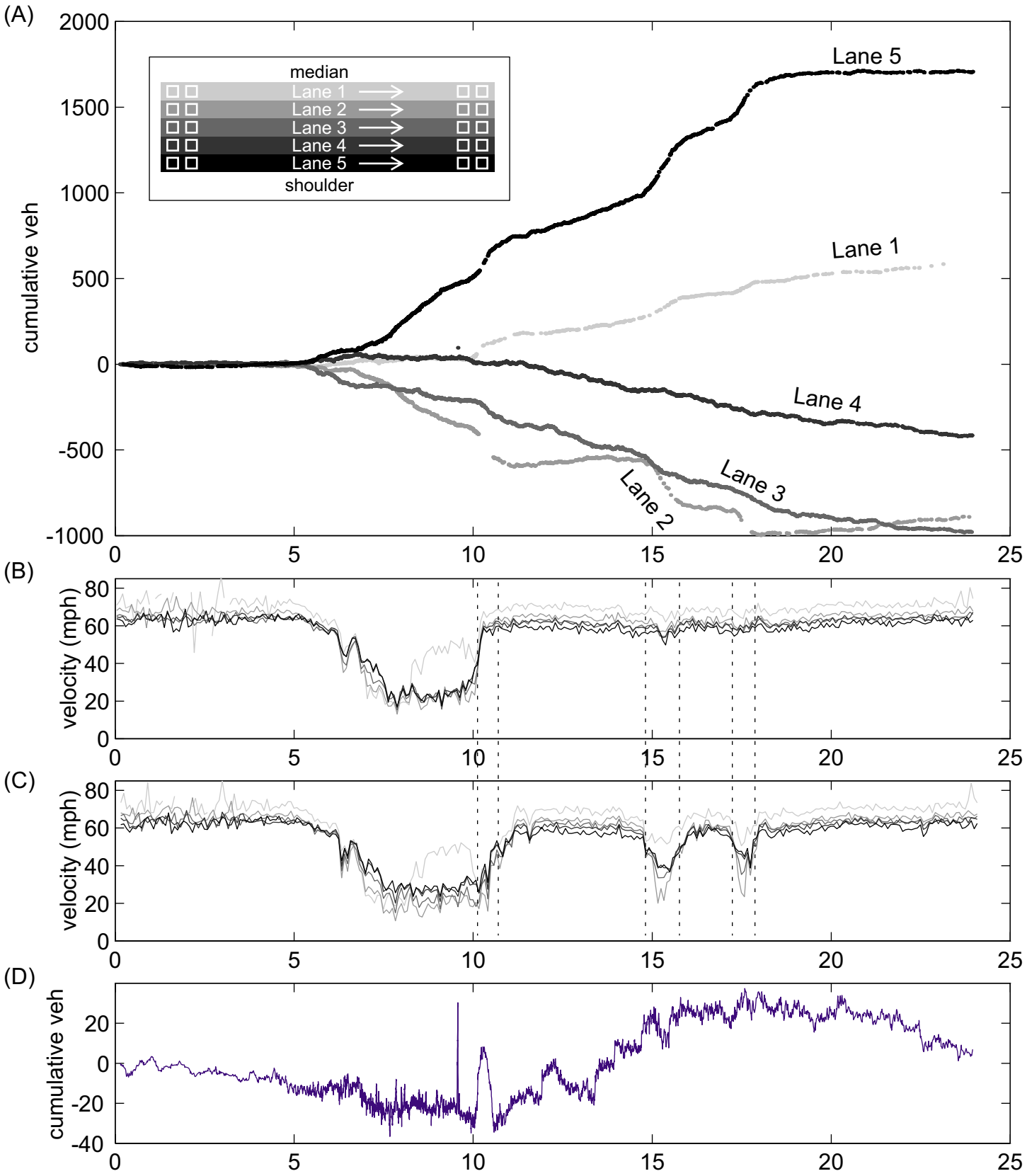

5 ACKNOWLEDGMENTS

The authors would like to acknowledge the input, contributions and support from Edgar Ergueta at the University of California, Berkeley, Bonny Banerjee at the Ohio State University, as well as Joe Palen, Sean Coughlin, Ron Slade, and Judy Chen at Caltrans.

6 REFERENCES

Balke, K., Ullman, G., McCasland, W., Mountain, C., Dudek, C. (1995). *Benefits of Real-Time Travel Information in Houston, Texas*, Southwest Region University Transportation Center, Texas Transportation Institute, College Station, TX.

Chang, G., Kao, Y. (1991) "An Empirical Investigation of Macroscopic Lane-Changing Characteristics on Uncongested Multilane Freeways", *Transportation Research- Part A*, Vol 25A, No 6, pp 375-389.

Chang, M., Gazis, D. (1975). "Traffic Density Estimation with Consideration of Lane-Changing", *Transportation Science*, Vol 9, No 4, pp 308-320.

Coifman, B. (1998). *Vehicle Reidentification and Travel Time Measurement Using Loop Detector Speed Traps*, Dissertation, University of California.

Coifman, B. (1999). "Using Dual Loop Speed Traps to Identify Detector Errors", *Transportation Research Record no. 1683,* Transportation Research Board, pp 47-58.

Coifman, B., Lyddy, D., and Skabardonis, A. (2000). "The Berkeley Highway Laboratory-Building on the I-880 Field Experiment", *Proc. IEEE ITS Council Annual Meetin*g, pp 5-10.

Coifman, B. (2001). "Improved Velocity Estimation Using Single Loop Detectors" *Transportation Research: Part A*, vol 35, no 10, pp. 863-880, Elsevier Science, London.

Coifman, B. (2002). "Estimating Travel Times and Vehicle Trajectories on Freeways Using Dual Loop Detectors", *Transportation Research Part A*, vol 36, no 4, pp. 351-364..

Coifman, B. and Cassidy, M. (in press). "Vehicle Reidentification and Travel Time Measurement on Congested Freeways", *Transportation Research-A*. Draft available at: http://www-ceg.eng.ohio-state.edu/~coifman/documents

Coifman, B. (in press). "Identifying the Onset of Congestion Rapidly with Existing Traffic Detectors", *Transportation Research-A*. Draft available at: http://www-ceg.eng.ohio-state.edu/~coifman/documents

Coifman, B., Dhoorjaty, S., and Lee, Z. (*in press*). "Estimating Median Velocity Instead of Mean Velocity at Single Loop Detectors", *Transportation Research-Part C*. Draft available at: http://www-ceg.eng.ohio-state.edu/~coifman/documents

Coifman, B. (*in press*). "Identifying the Onset of Congestion Rapidly with Existing Traffic Detectors", *Transportation Research-Part A*. Draft available at: http://www-ceg.eng.ohio-state.edu/~coifman/documents

Cui, Y., Huang, Q. (1997). "Character Extraction of License Plates from Video" *Proc. 1997 IEEE Computer Society Conference on Computer Vision and Pattern Recognition*, IEEE, pp 502-507.

Dailey, D. (1993). "Travel Time Estimation Using Cross Correlation Techniques", *Transportation Research-Part* B, Vol 27, No 2, pp 97-107.

Edie, L. (1963). "Discussion of traffic stream measurements and definitions", *Proc. Second International Symposium on the Theory of Traffic Flow*, OECD, Paris, France, pp 139-154.

Gazis, D., Knapp, C. (1971). "On-line Estimation of Traffic Densities from Time-Series of Flow and Speed Data", *Transportation Science*, Vol 5, pp 283-301.

Gazis, D., Szeto, M. (1974). "Design of Density-Measuring Systems for Roadways", *Transportation Research Record 495*, Transportation Research Board, pp 44-52

Greenshields, B. (1934). "The Photographic Method of Studying Traffic Behavior", *Highway Research Board Proceedings*, Vol 13, pp 382- 399

Greenshields, B. (1935). "A Study of Traffic Capacity", *Highway Research Board Proceedings*, Vol 14, pp 448-477

Holdener, D., Turner, S. (1996). "Probe Vehicle Sample Sizes for Real-Time Information: the Houston Experience", *Intelligent Transportation: Realizing the Benefits- Proc. Of the 1996 Annual Meeting of ITS America*, Vol 1, ITS America, pp 287-295.

Huang, T., Russell, S. (1997). "Object Identification in a Bayesian Context", *Proceedings of the Fifteenth International Joint Conference on Artificial Intelligence (IJCAI-97*), Nagoya, Japan.

Kuhne, R., Immes, S. (1993). "Freeway Control Systems for Using Section-Related Traffic Variable Detection", *Pacific Rim TransTech Conference Proc., Vol* 1, ASCE, pp 56-62.

Larson, J., Van Katwyk, K., Liu, C., Cheng, H., Shaw, B., Palen, J. (1998). *A Real-Time Laser-Based Prototype Detection System for Measurement of Delineations of Moving Vehicles*. UCB-ITS-PWP-98-20, PATH, University of California, Berkeley, CA.

Lighthill, M., Whitham, G. (1955). "On Kinematic Waves II. A Theory of Traffic Flow on Long Crowded Roads", *Proc. Royal Society of London, Part A*, vol 229, no 1178, pp 317-345.

Lin, W., Daganzo, C. (1997) "A Simple Detection Scheme for Delay-Inducing Freeway Incidents", *Transportation Research-Part A*, Vol 31A, No 2, pp 141-155.

MacCarley, C. A. (1998). *Videobased Vehicle Signature Analysis and Tracking Phase 1: Verification of Concept and Preliminary Testing*. UCB-ITS-PWP-98-10, PATH, Univeristy of California, Berkeley, CA.

Munjal, P., Hsu, Y. (1973). "Experimental Validation of Lane-Changing Hypotheses From Aerial Data", *Highway Research Record 456*, pp 8-19

Nahi, N., Trivedi, A. (1973). "Recursive Estimation of Traffic Variables: Section Density and Average Speed", *Transportation Science*, Vol 7, pp 269-286.

Pahl, J. (1972). "Lane-Change Frequencies in Freeway Traffic Flow", *Highway Research Record 409*, pp 17-25

Palen, J. (1997). "The Need for Surveillance in Intelligent Transportation Systems", *Intellimotion*, Vol 6, No 1, University of California PATH, Berkeley, CA, pp 1-3, 10.

Petty, K., Bickel, P., Ostland, M., Rice, J., Schoenberg, F., Jiang, J., Ritov, Y. (1997). "Accurate Estimation of Travel Times From Single Loop Detectors", *Transportation Research-Part* A, Vol 32, No 1, pp 1-17.

Pfannerstill, E. (1984). "A Pattern Recognition System for the Re-identification of Motor Vehicles", *Proc. 7th International Conference on Pattern Recognitio*n, Montreal, IEEE, New Jersey, pp 553-555.

Reijmers, J. (1979). "On-Line Vehicle Classification", *Proceedings of the International Symposium on Traffic Control System*s, Vol 2B, Institute of Transportation Studies, University of California at Berkeley, pp 87-102.

Richards, P. (1956). "Shock Waves on the Highway", *Operations Research*, 4 (1), pp 42-51.

Skabardonis, A., Petty, K., Noeimi, H., Rydzewski, D. and Varaiya, P. (1996). "I-880 Field Experiment: Data-Base Development and Incident Delay Estimation Procedures", *Transportation Research Record 1554*, Transportation Research Board, pp 204-212.

Sheu, J. (1999). "A Stochastic Modeling Approach to Dynamic Prediction of Section-Wide Inter-Lane and Intra-Lane Traffic Variables Using Point Detector Data", *Transportation Research Part A*, Vol 33A, pp 79-100.

Van Aerde, M., Hellinga, B., Yu, L., Rakha, H. (1993). "Vehicle Probes as Real-Time ATMS Sources of Dynamic O-D and Travel Time Data", *Large Urban Systems- Proc. Of the Advanced Traffic Management Conference*, FHWA, pp 207-230.

Westerman, M., Immers, L. (1992). "A Method for Determining Real-Time Travel Times on Motorways", *Road Transport Informatics/Intelligent Vehicle Highways System*s, ISATA, pp 221-228.

Westerman, M., Litjens, R., Linnartz, J. (1996). *Integration of Probe Vehicle and Induction Loop Data- Estimation of Travel Times and Automatic Incident Detectio*n. PATH, University of California at Berkeley.

Worrall, R., Bullen, A. (1970). "An Empirical Analysis of Lane Changing on Multilane Highways", *Highway Research Record 303*, pp 30-43.

Worrall, R., Bullen, A., Gur, Y. (1970). "An Elementary Stochastic Model of Lane-Changing on a Multilane Highway", *Highway Research Record 308*, pp 1-12